Comparative Analysis of the Quantization of Color Spaces on the Basis of the CIELAB Color-Difference Formula

B. HILL, Th. ROGER, and F. W. VORHAGEN
Aachen University of Technology

This article discusses the CIELAB color space within the limits of optimal colors including the complete volume of object colors. A graphical representation of this color space is composed of planes of constant lightness L^* with a net of lines parallel to the a^* and b^* axes. This uniform net is projected onto a number of other color spaces (CIE XYZ, tristimulus RGB, predistorted RGB, and YCC color space) to demonstrate and study the structure of color differences in these spaces on the basis of CIELAB color difference formulas. Two formulas are considered: the CIE 1976 formula ΔE_{ab} and the newer CIE 1994 formula ΔE^*_{94}. The various color spaces considered are uniformly quantized and the grid of quantized points is transformed into CIELAB coordinates to study the distribution of color differences due to basic quantization steps and to specify the areas of the colors with the highest sensitivity to color discrimination. From a threshold value for the maximum color difference among neighboring quantized points searched for in each color space, concepts for the quantization of the color spaces are derived. The results are compared to quantization concepts based on average values of quantization errors published in previous work. In addition to color spaces bounded by the optimal colors, the studies are also applied to device-dependent color spaces limited by the range of a positive RGB cube or by the gamut of colors of practical print processes (thermal dye sublimation, Chromalin, and Match Print). For all the color spaces, estimations of the number of distinguishable colors are given on the basis of a threshold value for the color difference perception of $\Delta E_{ab} = 1$ and $\Delta E^*_{94} = 1$.

Categories and Subject Descriptors: G.1.2 [**Numerical Analysis**]: Approximation; I.3.1 [**Computer Graphics**]: Hardware Architecture; I.3.3 [**Computer Graphics**]: Picture/Image Generation—*display algorithms*; I.3.7 [**Computer Graphics**]: Three-Dimensional Graphics and Realism—*color, shading, shadowing, and texture*; I.4.1 [**Image Processing**]: Digitization—*quantization*

General Terms: Algorithms, Experimentation, Performance, Standardization

Additional Key Words and Phrases: CIE XYZ, CIELAB, CIELAB color space, CIELUV, color difference perception, color quantization, color spaces, Cromalin, dye sublimation printer, match print, optimal colors, RGB, YCC

Authors' address: Aachen University of Technology, RWTH, Templergraben 55, Aachen 52056, Germany.

1. INTRODUCTION

The CIELAB color space is one of the approximately uniform color spaces recommended for device-independent color representation in electronic color image systems. Color as part of the information of a document is described at less redundancy in CIELAB dimensions than in linear RGB or XYZ primary color systems and it has therefore been introduced into Postscript language and Photoshop and is increasingly used and accepted in all kinds of professional and commercial imaging systems for color representation.

If colors are represented by the CIELAB space, the axes of lightness L^* and chromaticities a^* and b^* have to be suitably quantized. Therefore the range of colors and the limitations of the axes have to be specified. The standardized CIELAB definition [CIE 1986a] gives a limit only for the L^* axis ($0 \leq L^* \leq 100$) whereas no limitations are specified for a^* and b^*. As far as object colors are concerned, a theoretical limitation is given by the so-called optimal colors derived from the limited spectral reflectance or transmission curves together with a specified illuminant [Schrödinger 1920; Rösch 1929; MacAdam 1935a, b]. A color space with the surface of optimal colors includes all the smaller color gamuts in technical reproductions.

The primary aim of this article is to describe the gamut of optimal colors in a specified grid of the CIELAB space and to make evident how this gamut and grid of colors represents itself if it is transformed into a number of other typical color spaces. Therefore the CIELAB optimal color space [CIE 1986b], the CIE XYZ [CIE 1986c], the RGB [CCIR 1982], and the Kodak YCC color spaces [Kodak 1992] with the gamut of optimal colors are represented in graphical form.

These representations also show clearly the principal structure of the CIELAB space compared to other color spaces. If cells of cubic form in various parts of the CIELAB space are transformed into other color spaces such as the XYZ or RGB space, they become deformed and in some cases strongly compressed. These deformations demonstrate the differing sensitivities of color perception as a function of the coordinates among the different color spaces and within each color space.

The colors in technical reproduction systems cover a smaller gamut than those of optimal colors. To demonstrate the typical differences, the tristimulus and predistorted RGB space with positive components between 0 and 100 only (ITU-R BT.709, formerly CCIR 709), the Kodak YCC space with standard specification [Kodak 1992], and the device-dependent color spaces of a thermal dye sublimation printer, and the Chromalin proofing system are presented in CIELAB coordinates.

A last aim of this article is to compare the quantization of the various color spaces examined. Therefore the same quantization concept is applied to the various color spaces without matching the quantization to a special application. This has the advantage that specific differences among the color spaces can be exposed. The quantization is based on the CIELAB color

difference formulas. The most common formula was published in 1976 [CIE 1986a]. An improved formula was recommended by the CIE Technical Committee 1-29 in 1994 [Alman 1993; CIE 1993]. Both formulas are used as a basis for quantization and we outline the essential differences resulting from the different structures of the formulas.

Quantization concepts have already been discussed in other papers. In Kasson and Plouffe [1992], a number of test colors within the range of real surface colors as given by Pointer [1980] are defined for three levels of lightness in the CIELUV space. An arbitrary number of sample points around the test points defines shifted colors used to calculate small color differences. These points are then transformed into a color space to be studied and they are quantized in this space assuming an 8-bit quantization per axis. Then the quantized points are transformed back into the source color space and compared with the exact points not being quantized. The resulting differences provide transformed quantization errors. From these, an average error over all the test points and the statistical three-sigma error is calculated in terms of the CIELUV—as well as the CIELAB—color difference definitions ΔE_{uv} and ΔE_{ab}. The result of the average error is finally expressed as the average value from both color difference definitions, whereas the maximum of both is used for the average three-sigma error. As a typical result, the quantization of 8 + 8 + 8 bits yields an average three-sigma error of 0.5 for the quantization of the CIELUV space, 0.4 for the CIELAB space, and 4.1 for the CIE XYZ space, respectively. Reduction of the error by a factor of 2 requires approximately 1 bit more per component, which means, for example, that 10 bits per component are necessary to come to an error close to $\Delta E = 1$ for the quantization of the CIE XYZ space.

An experimental method to estimate a useful quantization was published in Stokes et al. [1992a]. Perceptibility experiments at pictorial images reproduced on a high quality display were performed to derive perceptibility tolerances expressed in ΔE_{ab} units. A variety of typical color manipulations was applied to a large number of images of different types. Finally, an average perceptibility threshold of $\Delta E_{ab} = 2.15$ was found. From this result, the minimum quantization of 6.4 bits for the L^* axis and 7.1 bits for the a^* and b^* axes of the CIELAB space are specified. For the quantization of a nonlinear RGB CRT color space, 7.4 bits per component are derived.

In Mahy et al. [1991], quantization errors in an RGB color space for an 8-bit quantization have been calculated and transformed into CIELAB, CIELUV, and ATD color spaces. Maximum and mean errors are outlined for grey values (equal components of RGB). Large differences among the errors were found for high and low grey values and among the different components of the color spaces. From experiments with displayed images, a perceptable threshold value of $\Delta E_{ab} = 1$ was found for the lightness and 3 for chroma values a^* and b^*.

In this article, maximum color quantization steps of a number of color spaces instead of mean errors are calculated for all possible directions of quantized steps in three-dimensional spaces and for all the positions within

each space. Maximum color quantization steps provide a "worst case" basis for the estimation of necessary quantization concepts. Those concepts are outlined for the CIELAB, CIELUV, and CIE XYZ device-independent color spaces and the tristimulus and predistorted RGB space (ITU-R BT.709, formerly CCIR 709) within the limits of optimal colors [MacAdam 1935a, b] and for tristimulus and predistorted RGB spaces with positive components between 0 and 100 only, for the Kodak YCC space [Kodak 1992] and for device-dependent color spaces of a thermal dye sublimation printer and the Chromalin proofing system.

2. GENERAL CONCEPT OF THE ANALYSIS

2.1 CIELAB Color Space and Color Difference Formulas

The CIELAB system is a simplified mathematical approximation to a uniform color space composed of perceived color differences. The perceived lightness L^* of a standard observer is assumed to follow the intensity of a color stimulus according to a cubic root law [CIE 1986a]. The colors of lightness L^* are arranged between the opponent colors green-red and blue-yellow along the rectangular coordinates a^* and b^*. The total difference between the two colors is given in terms of L^*, a^*, b^* by the CIE 1976 formula

$$\Delta E_{ab} = \sqrt{\Delta L^{*^2} + \Delta a^{*^2} + \Delta b^{*^2}}.$$

Any color represented in the rectangular coordinate system of axes L^*, a^*, b^* can alternatively be expressed in terms of polar coordinates with the perceived lightness L^* and the psychometric correlates of chroma,

$$C_{ab}^* = \sqrt{a^{*^2} + b^{*^2}},$$

and hue angle,

$$h_{ab} = \tan^{-1}\left(\frac{b^*}{a^*}\right).$$

In fact, the CIELAB space is not really uniform. If MacAdam or Brown-MacAdam ellipses or ellipsoids are transformed into CIELAB coordinates, differences appear among their main axes of up to 1:6.

In particular, at high values of chroma, the simple CIE 1976 color difference formulas value color differences too strongly compared to experimental results of color perception [Loo and Rigg, 1987]. An improved color difference formula was therefore recommended in 1994 [Alman 1993; CIE 1993, 1995]:

$$\Delta E_{94}^* = \sqrt{\left(\frac{\Delta L^*}{k_L S_L}\right)^2 + \left(\frac{\Delta C_{ab}^*}{k_C S_C}\right)^2 + \left(\frac{\Delta H_{ab}^*}{k_H S_H}\right)^2},$$

where ΔL^*, ΔC^*_{ab}, and ΔH^*_{ab} are the CIELAB 1976 color differences of lightness, chroma, and hue; k_L, k_C, and k_H are factors to match the perception of background conditions; and S_L, S_C, and S_H are linear functions of C^*_{ab}. Color differences in this article have also been calculated for this formula and they are compared to the calculations for ΔE_{ab}. Standard reference values as specified in CIE [1993, 1995] have been assumed for the calculations of ΔE^*_{94}:

$$k_L = k_C = k_H = 1,\ S_L = 1$$

$$S_C = 1 + 0.045\ C^*_{ab},\ S_H = 1 + 0.015\ C^*_{ab}.$$

2.2 CIELAB Optimal Color Space

The volume of all the object colors that appear in nature is enclosed by the optimal colors with maximum saturation for a given lightness (Figure 1). A color space with the surface of the optimal colors therefore includes all the smaller gamuts of colors in technical reproductions using reflective or transmissive materials under a given illuminant [Schrödinger 1920; Rösch 1929; MacAdam 1935a, b].

Not included in the theory of color limitation by optimal colors are self-luminous colors. Nevertheless, the self-luminous colors of displays or other image sources can be included in a color space with the surface of optimal colors (hereafter called "optimal color space"), if the average lightness is clearly specified and matched to the average lightness of the surrounding scene. If, however, self-luminous colors are combined with reflective or transmissive colors in the same document, it has to be checked carefully whether the resulting colors are still represented in an optimal color space. Many printing papers with luminescent additions are problematic in this respect.

A comprehensive study of the gamut of colors has been given by Pointer [1980]. Film colors as well as real surface colors and their limits of maximum saturation are derived from experimental data and color books. As far as optimal colors are concerned, it has been proposed to use so-called "reduced optimal colors" instead of the theoretical values to take the finite optical density of reflective colors into account. This density is always limited by reflection and scattering of light at the surface of color pigments. When considering a maximum optical density of $D = 2.25$, the colors of maximum saturation are shifted by a few percent compared to the optimal colors with the theoretical density of infinity. Although the optical density limit of 2.25 is realistic for many prints, the limitation is very different for photographic transparencies and displays. To be independent of specific technologies, the absolute theoretical limits for optimal colors have been used in this article.

The CIELAB optimal color space bounded by the surface of the most saturated colors is shown in Figure 2. The space is composed of planes of constant lightness L^* that are arranged at distances of 5 units apart. Each plane is limited by the optimal colors of the respective lightness.

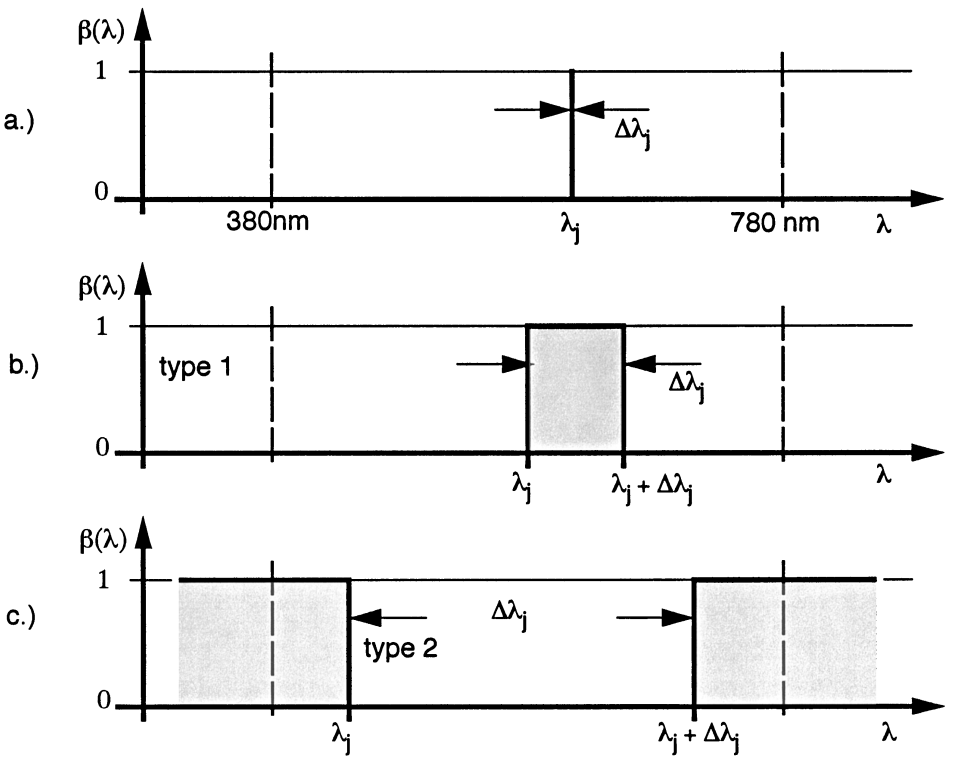

Fig. 1. Remission curves of a spectral object color (a), an optimal color type 1 (b), and an optimal color type 2 (c). An optimal color is an object color with the spectral remission occupying only the two extreme values $\beta(\lambda) = 1$ or $\beta(\lambda) = 0$ and with, at a maximum, only two steps between these values. Each optimal color is the most saturated color of given chromaticity at a given lightness. Two types of optimal colors are possible, one with the remission curve occupying a continuous range $\Delta\lambda_1$ of the spectrum (type 1) and another occupying two separate ranges (type 2) with single steps.

The calculation of these color planes starts from a CIE Y_i value according to a given lightness L_i^*. For type 1 optimal colors (see Figure 1), the equation

$$Y_i(\lambda_j, \Delta\lambda_{i,j}) = K \cdot \int_{\lambda_j}^{\lambda_j + \Delta\lambda_{i,j}} S_\lambda \cdot \bar{y}(\lambda) d\lambda; \quad K = \frac{100}{\int_{380\text{ nm}}^{780\text{ nm}} S_\lambda \cdot \bar{y}(\lambda) d\lambda}$$

has to be solved as a function of $\Delta\lambda_{i,j}$ for each value of λ_j. The function $\bar{y}(\lambda)$ is the spectral matching curve of the CIE XYZ system.

An equal-energy flux $S_\lambda = 1$ has been assumed for the calculation of the general color spaces CIELAB and CIE XYZ, and S_λ according to the illuminant D65 has been considered for specific color spaces in RGB or YCC components. Starting from a specific value of the lightness L^* transferred to Y_i, the integral equation results in a value $\Delta\lambda_{i,j}$ for each value of λ_j. For

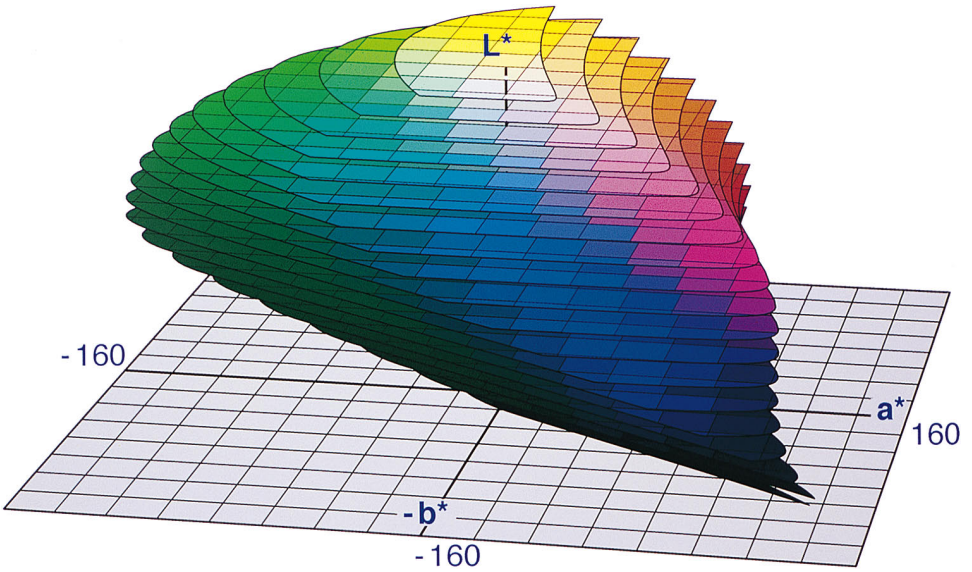

Fig. 2. CIELAB optimal color space composed of planes of constant lightness L^* spaced $\Delta L^* = 5$ units. The net indicated in each plane represents lines of constant a^* or b^* with line spacings of 20 units.

the results shown in Figure 2, the wavelength λ_j has been varied in steps of 1 nm throughout the visible spectrum. The same procedure is applied to type 2 optimal colors as well. With the integration limits found, the accompanying X and Z optimal color values are determined:

$$X_{i,j} = K \cdot \int_{\lambda_j}^{\lambda_j+\Delta\lambda_{i,j}} S_\lambda \cdot \bar{x}(\lambda)d\lambda, \quad Z_{i,j} = K \cdot \int_{\lambda_j}^{\lambda_j+\Delta\lambda_{i,j}} S_\lambda \cdot \bar{z}(\lambda)d\lambda.$$

All the results of color values $X_{i,j}$, Y_i, and $Z_{i,j}$ are lined up for each particular value of Y_i, interpolated, and converted to the L^*, a^*, b^* values that describe the border line of a plane L_i^* in Figure 2.

The optimal color space shows some typical characteristics. The lower planes are stretched out into the blue range forming a slim "nose." At higher lightness, the center of the planes moves from blue towards yellow. At low lightness, blue colors are dominant. At medium lightness, a maximum number of perceivable colors is achieved and at high lightness, only yellow and green colors are present.

Figure 3 shows a top view of the CIELAB optimal color space for equal energy flux $S_\lambda = 1$ according to the light source demonstrating the overall dimensions in the a^*-, b^*-plane. The CIELAB optimal color space is thus arrayed within the limits $0 \le L^* \le 100$; $-166 < a^* < 141$; $-132 < b^* < 147$.

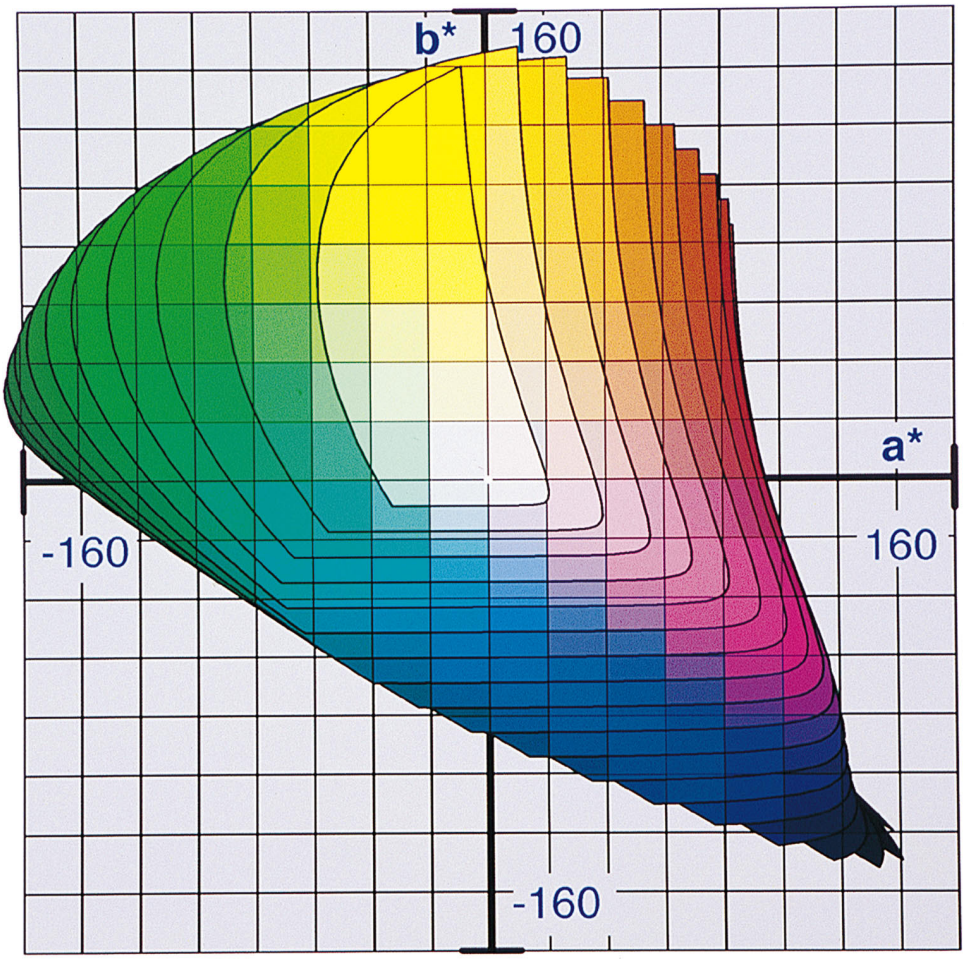

Fig. 3. Top view on the CIELAB optimal color space. The uppermost plane corresponds to the lightness of $L^* = 95$. $L^* = 100$ gives the white point.

2.3 CIELAB Color Difference Formula, Just-Noticeable Color Difference, and Number of Bits

For quantizing color spaces, a threshold value of color differences has to be defined. Although many studies have dealt with this problem, a clear threshold definition has not been given up to now. A first problem is that the CIELAB space is not really uniform and that therefore the perception of color differences changes with the location of colors within the color space and with the direction in the color space.

Another problem is that the just-noticeable threshold depends on the kind of image and the ambient illumination. An extensive experimental study on perceptibility tolerances of pictorial images reproduced on CRTs has shown that the average perceptible difference lies in the range of $\Delta E_{ab} \approx 1.57$ to 2.56 [Stokes et al. 1992a]. On average, a color difference of

$\Delta E_{ab} \approx 1$ would not be noticed in electronic images after these experiments. The experiments published in Mahy et al. [1991], Schwarz et al. [1987], and Stokes et al. [1992b] result in the same order of magnitude of perceptibility thresholds between 1 and 3 for practical images. In professional or electronic prints, the uncertainty of color reproduction is typically of the order of several units of ΔE_{ab}. On the other hand, color difference thresholds of much below $\Delta E_{ab} \approx 1$ are required in some fields of industrial coloring, when comparing, for example, colors of cars or textiles [SAE 1985]. In this article, thresholds of $\Delta E \approx 1$ or $\Delta E^*_{94} \approx 1$ have been assumed as a worthwhile basis for quantization in view of the requirements in electronic imaging. For complex computing of colors, it may be necessary to use lower quantization thresholds than for the reproduction of a final image because quantization errors add up in a series of calculations [Stokes et al. 1992b]. If required, the results derived in this article can be approximately converted to lower or higher limits of the threshold of ΔE according to the relation that 1 bit more for all 3 color components reduces the color quantization threshold by the factor 2 and vice versa. Thus the results shown in this article can be matched to differing requirements of practical engineering problems. If a bit number is derived from a just-noticeable difference of ΔE along an axis with the range ΔQ in the following, the number of N bits of quantization is defined as the smallest integer number that keeps the quantization steps just below or equal to the number ΔE according to the equation:

$$\frac{\Delta Q}{2(N/[bit])} \leq \Delta E \leq 1.$$

2.4 The General Concept for Defining a Quantization Box

In most cases, the color gamut of a color space shows a quite complicated form. In order to describe the colors within the gamut by a linear binary code with three independent components, the color gamut is first placed within the smallest rectangular box (hereafter called "quantization box"). The edges of the box are chosen parallel to the axes of the color space being quantized. The three dimensions of the box define the ranges of the axes to be quantized in order to catch any color within the gamut. For the case of the CIELAB space of Figures 2 and 3, for example, the box must have the dimensions 100 units along the L^* axis, 307 along the a^* axis, and 279 along the b^* axis.

In a second step, quantization intervals are defined for each axis assuming the full range of steps along each axis to be described by a digital word of a specific length. For the case of the CIELAB space, these quantization intervals are $100/2^8 = 0{,}392$ for an 8-bit quantization of the L^* axis, $307/2^9 = 0{,}601$ for the 9-bit quantization of the a^* axis, and $279/2^9 = 0{,}546$ for a 9-bit quantization of the b^* axis.

The assumed quantization defines a uniform grid of color points in any of the considered color spaces. Each digital step from one point of the grid to

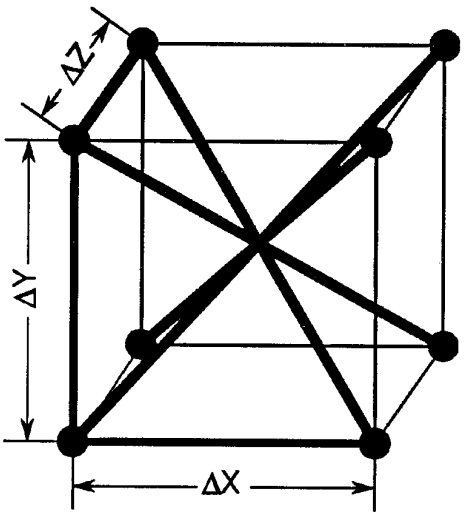

Fig. 4. Quantization cell used to determine the maximum color difference ΔE_{ab} for the digitization of an arbitrary color space. The color difference ΔE_{ab} is calculated for each combination of minimum quantization steps $\pm\Delta$X, $\pm\Delta$Y, and $\pm\Delta$Z. The maximum color difference for these combinations is often found for one of the steps between opposing edge points of the cell if digital steps $\pm\Delta$X, $\pm\Delta$Y, and $\pm\Delta$Z are changed at once. Four of those diagonal steps through the cell are possible and result in different color differences in many cases.

one of the neighbors produces a color difference. By converting the grid of an arbitrary color space into CIELAB coordinates, the color difference can be calculated in ΔE_{ab} or ΔE^*_{94} units.

A basic cell of adjacent color points of the grid in an arbitrary color space is sketched in Figure 4. When switching digitally from one quantized value of an axis to the next, or when doing the same at two or three axes altogether, there are seven possible steps of producing different color differences among neighboring color points: three along the axis (ΔX, ΔY, ΔZ in Figure 4) and four diagonally through the cell. In a nonuniform color space all seven steps might produce different color differences.

Normally, one of the diagonal steps produces the maximum color difference. This is called the worst color quantization step $\Delta E_{ab,\mathrm{worst}}$ at the point checked. It is the aim of this study to search for this maximum of $\Delta E_{ab,\mathrm{worst}}$ for all the color points of a color space looked at and to find a quantization concept that keeps this maximum $\Delta E_{ab,\mathrm{max}}$ below an assumed threshold. If the maximum for a given quantized grid in the beginning is found to be still higher than the assumed threshold, the resolution of the quantization is increased until the goal is reached. In general, only round bit numbers are considered. This means that the final maximum color difference might be one in a limit or somewhat smaller due to rounding up the bit numbers.

For the case of the quantization of the CIELAB space according to the CIE 1976 formula, the search is simple since the grid of color distances is assumed to be uniform by itself and hence, the largest diagonal distance through the quantization cell gives the largest ΔE_{ab}. Assuming the quantiza-

tion of ($L^* + a^* + b^*$) = 8 + 9 + 9 integer bits, the maximum results in $\Delta E_{ab,\max} = 0{,}9$.

For nonuniform spaces, a more complicated algorithm to find the maximum is required. An operator is therefore moved throughout the complete gamut of colors and at each position, all seven directional steps according to the quantization cell (Figure 4) are checked for the maximum value of color difference.

3. QUANTIZATION OF THE OPTIMAL COLOR SPACE IN CIELAB COORDINATES AND THE NUMBER OF DISTINGUISHABLE COLORS

As outlined in the previous section, the maximum color difference step is the longest diagonal through the basic quantization cell expressed in ΔE units. With the assumed dimensions of the quantization box put around the optimal color gamut, the following concept results:

Component	Range	Quantization	Digitization
a^*	$-166 \rightarrow 141$	0,6008	9 bit
b^*	$-132 \rightarrow 147$	0,5460	9 bit
L^*	$0 \rightarrow 100$	0.3922 (0.7874)	8 bit (7 bit)
		sum	26 bit (25 bit)

The maximum is $\Delta E_{ab\max.} = 0.9$ for this concept. Using seven bits for the L^* axis would result in a maximum $\Delta E_{ab\ \max.}$ of 1.13.

With the just-noticeable color difference threshold assumed to be of the order of 1, a rough estimation of the number of distinguishable colors can be derived from the value of the color gamut. If the volume is assumed to be composed of cubes with $\Delta L^* = \Delta a^* = \Delta b^* = 1$, then $2.29 \cdot 10^6$ cubes are found. A better approximation to the number of distinguishable colors is achieved if the volume is assumed to be filled with balls of the diameter of $\Delta E_{ab} = 1$. This results in $3.24 \cdot 10^6$ colors. Experimentally, the number of distinguishable surface colors has been found to be 2 to $4 \cdot 10^6$ in good agreement with this result [Richter 1979]. If the higher threshold value of $\Delta E_{ab} = 2$ had been assumed, the bit numbers would have been 8 + 8 + 7 (see remarks in Section 2.3 concerning the change of the threshold).

4. THE OPTIMAL COLOR SPACE TRANSFORMED INTO SOME TRISTIMULUS SYSTEMS

Next we show graphical representations of the uniform grid of colors of the CIELAB space when being transformed into the primary color spaces CIE XYZ and RGB. In addition, the quantization of the CIE XYZ and RGB spaces is studied by assuming a uniform grid in these spaces and calculating the resulting maximum color quantization steps in terms of CIELAB units.

4.1 CIE XYZ Primary Color System

The projection of the CIELAB optimal color space with the planes of constant lightness as shown in Figure 2 into the CIE XYZ system is plotted

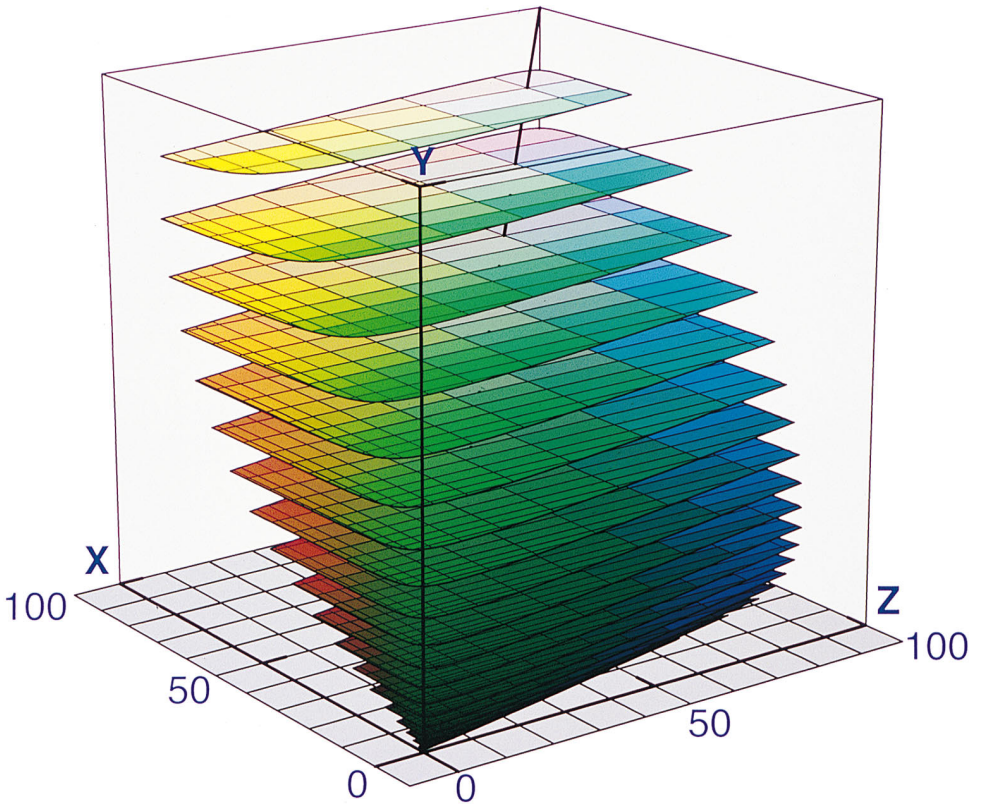

Fig. 5. XYZ optimal color space composed of planes of constant Y values arranged at luminance differences according to $\Delta L^* = 5$. The straight lines within each plane represent the lines of constant a^* values (parallel to the X axis) and lines of constant b^* values (parallel to the Z axis). The lines are arranged at distances according to 20 Δa^* or 20 Δb^* units. An illuminant of equal energy flux has been assumed.

in Figure 5. The Y axis is computed using only the L* coordinate. Due to the cubic root law of this transformation, the planes located every five units along the L^* axis in the CIELAB space are now compressed very close together at low Y values and they drift apart at higher Y values. The lines of constant b^* (see Figure 5) within each plane are imaged into lines parallel to the X axis and the lines of constant a^* parallel to the Z axis, respectively. The squares of 20×20 ΔE_{ab}-units formed by crossed lines a^* and b^* in Figure 3 are imaged into rectangles of very different size and area in each plane of the XYZ system. The smallest rectangles appear in the green area, where the sensitivity of color discrimination with changes of X or Z is largest. It is generally found that the most sensitive areas with respect to color discrimination are located at the border of the optimal colors.

To gain more insight into the structure of nonuniformity and color differences, the CIE XYZ space has been quantized using 10 bits per component. The smallest possible quantization box surrounding the opti-

mal colors is used as a basis for these experiments. The resulting uniform grid of color points is then transformed into CIELAB coordinates where it becomes deformed. Then test points of the grid are considered and the color differences to all the neighboring points are calculated to select the maximum, which is called the worst color quantization step $\Delta E_{ab,\mathrm{worst}}$. In Figure 6 (top), $\Delta E_{ab,\mathrm{worst}}$ is plotted for the test points along the border of optimal colors of constant lightness L^* as a function of the hue angle h_{ab}. The lightness L^* is changed in steps of five units. It is shown that the worst $\Delta E_{ab,\mathrm{worst}}$ decreases with lightness L^*. As a function of the hue angle, broad maxima appear at low lightness L^* and small maxima at high lightness. The center of the maxima is shifted with L^* from green colors (~180° hue angle) to yellow colors (~90° hue angle).

The same study has been applied to the new color difference formula ΔE^*_{94}. The result at the bottom of Figure 6 again shows a typical trend in comparison to the top of the figure. The curves become smoother and peaks in the curves of $\Delta E_{ab,\mathrm{worst}}$ become flattened if color differences are valued by ΔE^*_{94}. This becomes understandable when one looks into the details of the contributions to color differences as a function of quantization steps in the CIE XYZ space. The peak of $\Delta E_{ab,\mathrm{worst}}$ at $L^* = 30$ and $h_{ab} = 180°$, for instance, is caused by a dominant change of chroma

$$\Delta C_{ab}{}^* = \Delta(\sqrt{a^{*^2} + b^{*^2}})$$

with 10-bit digital steps of ΔX, ΔY, and ΔZ in this case ($\Delta L^* = 0.24$, $\Delta C_{ab}{}^* = 5.2$, $\Delta H = 0.036$, $C_{ab}{}^* = 111$). In the CIE 94 formula, the high change of chroma is reduced by the factor of $1 + 0.0045 \cdot C_{ab}{}^*$, which is dominant in this case.

The maxima of $\Delta E_{ab,\mathrm{worst}}$ along lines of optimal colors are plotted as a function of L^* in Figure 7 (100% curve). To study the color quantization step for grid points inside the gamut of optimal colors, lines of test points "parallel" to the lines of optimal colors have been defined by reducing the chroma values to a fixed percentage of the chroma of the respective optimal color at each hue angle. The maximum quantization step $\Delta E_{ab,\mathrm{max}}$ for all hue angles of test points along such lines is then searched for and plotted versus the lightness L^* in Figure 7 (top). The percentage of chroma ranges from 0 to 100%. The value of 0% describes the result for test points along the neutral L^* axis. This result shows that there are strong differences between $\Delta E_{ab,\mathrm{max}}$-values for low and high lightness values when quantizing the colors in the CIE XYZ space. The maximum color difference in planes of high lightness is a factor of 20–25 smaller than in planes of low lightness. The $\Delta E_{ab,\mathrm{max}}$-values drop faster with L^* for low relative chroma values than for high ones. An important point is that the maximum color quantization error appears at the border of optimal colors (100% curve in Figure 7, top) and is located in the range of green to yellow colors (Figure 6, top).

The respective results for the CIE 1994 color difference formula are shown in Figure 7 (bottom). It is obvious that the increase of ΔE^*_{94} with

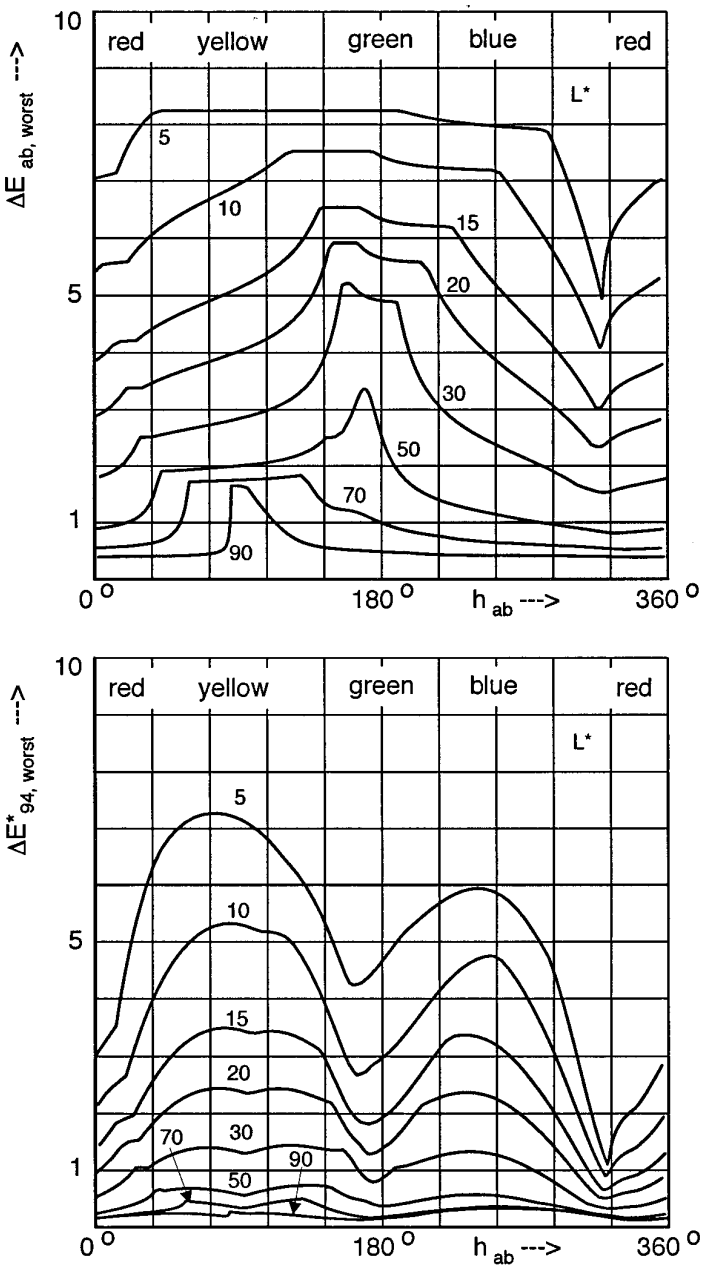

Fig. 6. Worst case color difference $\Delta E_{ab,\text{worst}}$ (top) and $\Delta E^*_{94,\text{worst}}$ (bottom) along lines of optimal colors at constant lightness L^* versus hue angle for the quantization in the CIE XYZ space (10 bits per axis). Parameter: lightness L^* (Illuminant C).

chroma is much smaller than for ΔE_{ab} due to the structure of the new formula that values chroma differences at high chroma less than those near the grey axis.

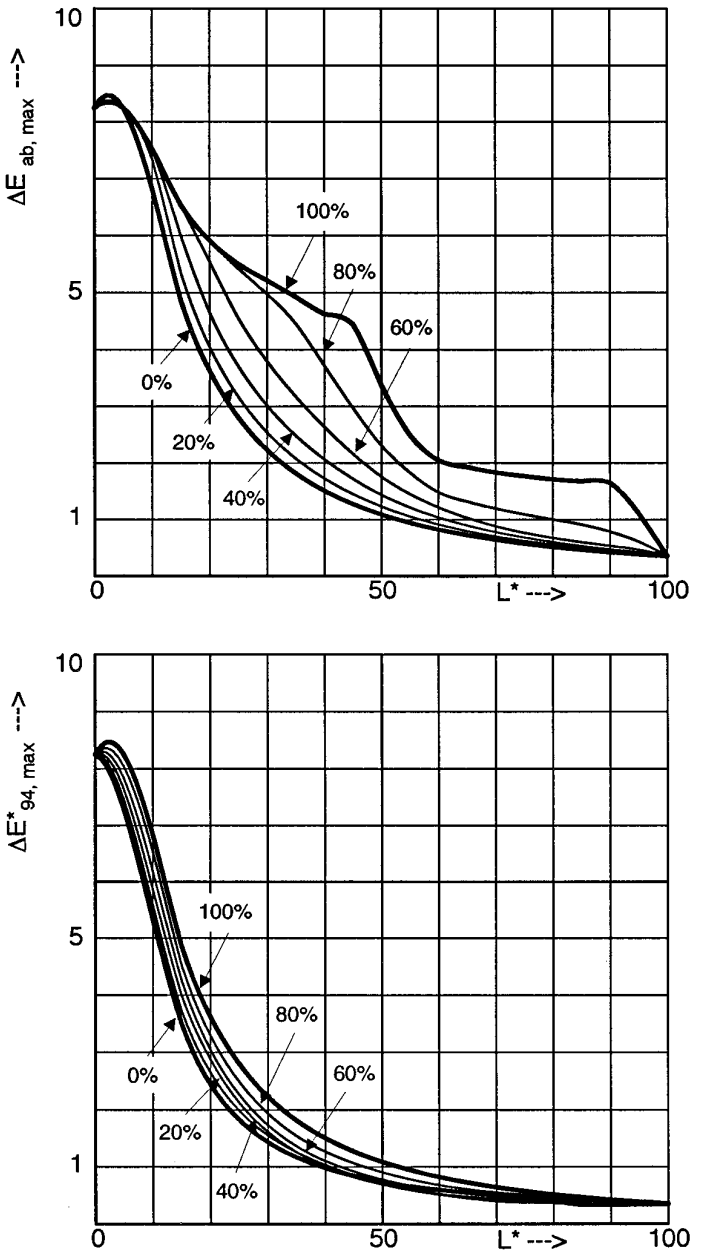

Fig. 7. Maximum color difference $\Delta E_{ab,\max}$ (top) and $\Delta E^*_{94,\max}$ (bottom) along lines of optimal colors (100%) at constant lightness L^* and lines with colors of reduced chroma given in % of the value of optimal colors vs. lightness level L^* for the CIE XYZ space (10 bits per axis).

As the color differences due to quantization in the CIE XYZ space vary greatly, it is not possible to define an optimal quantization concept. The concept with 10 bits per axis still produces quantization errors of more than

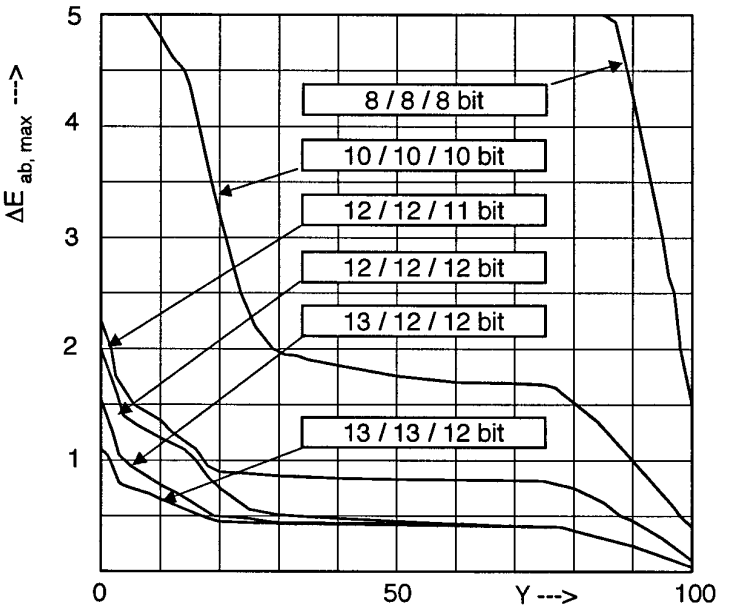

Fig. 8. Maximum color quantization steps $\Delta E_{ab,\max}$ vs. luminance component Y for various digitization concepts of the CIE XYZ optimal color space.

8 units of ΔE_{ab}. In Figure 8, the maximum color quantization step in a plane of constant lightness is plotted against the Y value for various quantization concepts. Even a concept with 12 bits per axis provides color differences above the assumed threshold of $\Delta E_{ab} = 1$ for Y values below 16 (corresponding to $L^* = 47$!). For the concept with 13 bits for the X and Y axis and 12 bits for the Z axis, the threshold is passed over for Y values below 1.1 (corresponding to $L^* = 10$). In a printed image, the Y values of 1 or 2 are produced by colorants of the optical density of 2 or 1.7, respectively. The optical density of 2 is close to the maximum achieved in practical image reproduction. If, therefore, the range of Y values from 1.1 to 100 (corresponding to $10 \leq L^* \leq 100$) is considered as a useful range, the quantization of the CIE XYZ space will be required to keep the color quantization steps $\Delta E_{ab,\max[L^* \geq 10]}$ just below 1.

Component	Range	Quantization Units (CIELAB-/CIE 94-formula)	Digitization for $\Delta E \approx 1$ (CIELAB-/CIE 94-formula)
X	$0 \rightarrow 100$	0.0122/0.0244	13 bit/12 bit
Y	$0 \rightarrow 100$	0.0122/0.0122	13 bit/13 bit
Z	$0 \rightarrow 100$	0.0244/0.0244	12 bit/12 bit
		sum	38 bit/37 bit

If the quantization is based on the CIE 94 formula, the results do not change significantly because the quantization is determined primarily by the differences of colors in the dark area in the CIE XYZ space, where

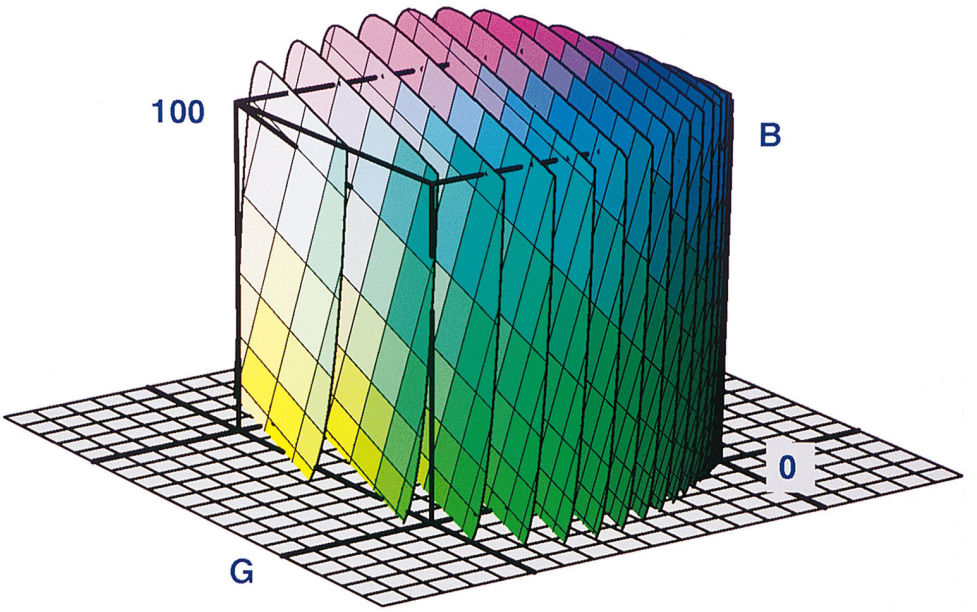

Fig. 9. Linear RGB optimal color space composed of planes of constant L^*-values with $\Delta L^* = 5$. The straight lines within each plane represent the lines of constant a^* values and lines of constant b^* values. Line spacing corresponds to $\Delta a^* = \Delta b^* = 20$ units. Values of $B < 0$ are not shown in the figure.

chroma values are small. Different illuminants have also little influence on the results.

4.2 Optimal Color Space in $RGB_{ITU\text{-}RBT}$-Coordinates

Most electronic image scanning, display, or printing equipment uses the tristimulus RGB system for color calculations in computer graphics or for control of printing devices at interfaces. As a standard, the ITU-R BT.709 (formerly CCIR 709) has been chosen in this article with white illuminant D65. The transformation for the CIE XYZ components to the RGB components is given by the following matrix equation.

$$\begin{bmatrix} R \\ G \\ B \end{bmatrix} = \begin{bmatrix} 3.0651 & -1.3942 & -0.4761 \\ -0.9690 & 1.8755 & 0.0415 \\ 0.0679 & -0.2290 & 1.0698 \end{bmatrix} \cdot \begin{bmatrix} X \\ Y \\ Z \end{bmatrix}.$$

Many systems also use RGB signals in compressed form, called γ distorted R′G′B′ signals. Colors represented in this distorted R′G′B′ coordinate system are discussed in the next section. The optimal colors for the linear RGB color space (also called RGB optimal color space) have been calculated and plotted in Figure 9. Again, the space is composed of planes of constant lightness L^* in steps of 5 ΔL^* units. The net of $a^* = $ const. and $b^* = $ const. according to a line spacing of 20 units is indicated as well. The RGB axes

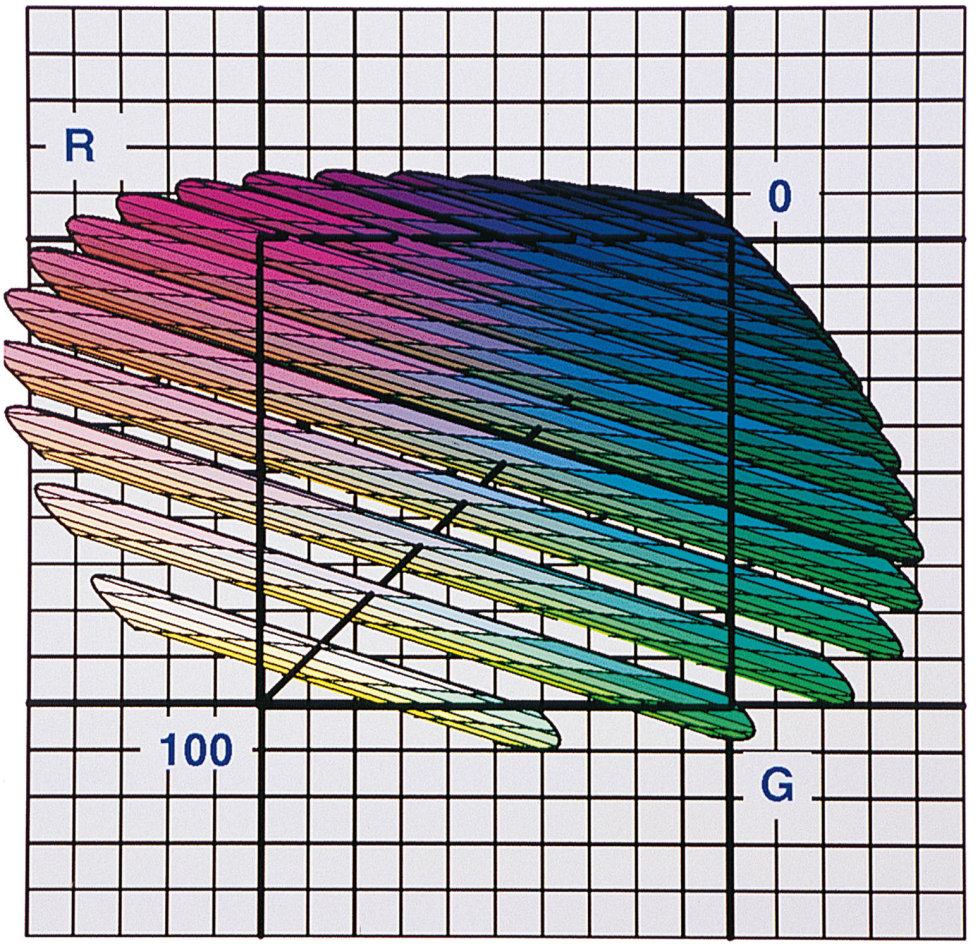

Fig. 10. View on the tristimulus RGB-optimal color space.

are normalized to 100 corresponding to the D65 XYZ values of (95.05, 100.0, 108.9).

Another view of the RGB optimal color space is given in Figure 10. These views demonstrate the dimensions of the space in negative and positive R- and G-directions.

The same method described in the previous sections has been applied to this space as well in order to evaluate the uniformity and quantization required to represent the complete volume of distinguishable colors. For studying uniformity, a uniform grid within a box around the complete tristimulus RGB color space was defined, assuming the quantization of 10 bits per axis. The respective ranges of the axes R, G, and B are given in Table III. Then the grid was transformed into the CIELAB space and maximum color differences between the adjacent points were calculated.

The dependence of the worst color quantization steps $\Delta E_{ab,\mathrm{worst}}$ on the hue angle h_{ab} for various lightness levels L^* at the border of optimal colors

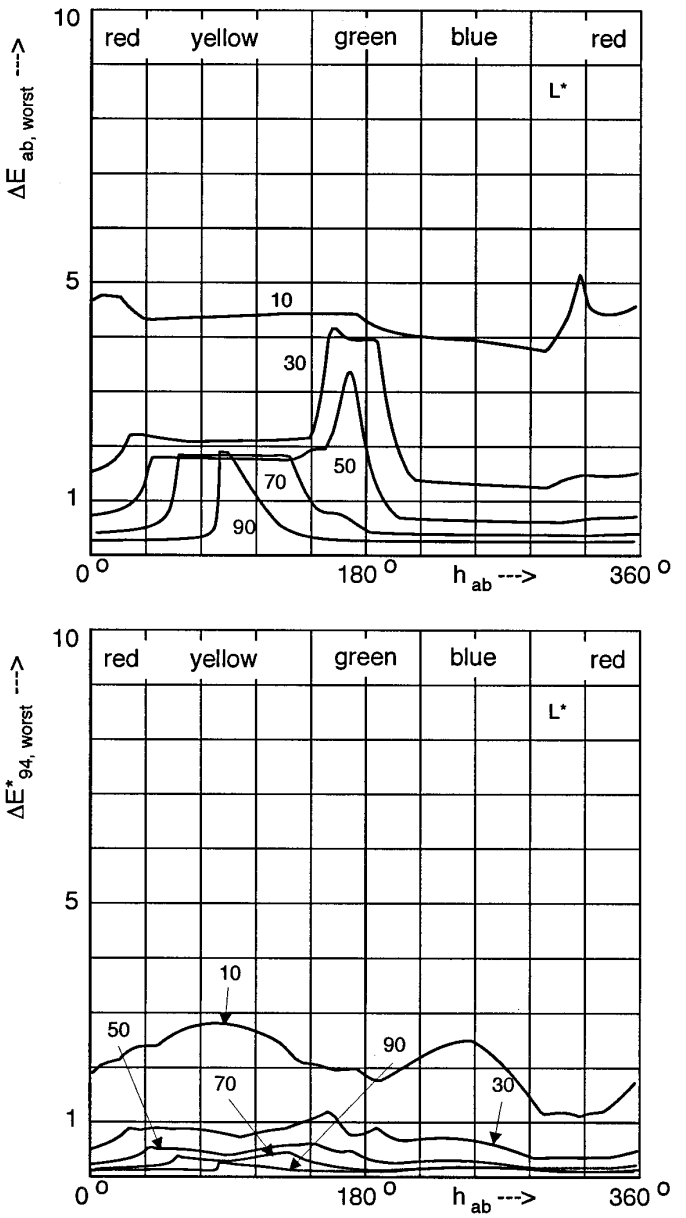

Fig. 11. Worst case color difference $\Delta E_{ab,\mathrm{worst}}$ (top) and $\Delta E^*_{94,\mathrm{worst}}$ (bottom) along lines of optimal colors at constant lightness L^* vs. hue angle for the quantization in the RGB space (10 bits per axis). Parameter: lightness L^* (Illuminant D65).

is plotted in Figure 11. At low lightness levels, the functions are quite uniform. At higher lightnesses, a maximum appears in the green range of colors (180°) moving towards yellow colors (90°) for highest lightness.

The respective results for the CIE 94 color difference formula are also given in Figure 11. All the curves of $\Delta E^*_{94,\mathrm{worst}}$ lie beyond the respective

curves of $\Delta E_{ab,\mathrm{worst}}$. The peaks in the green range of colors found for ΔE_{ab} have completely vanished. This is again due to the dominant influence of the change of chroma values of the green optimal colors which is reduced in ΔE^*_{94}.

The maximum color quantization steps of $\Delta E_{ab,\max}$ along the borderlines for various levels of L^* are given in Figure 12 as the 100% line. The curve shows two typical maxima at low lightness and medium lightness. The other curves for 80–0% show results for colors along lines of reduced chroma (given in percent of the respective values of optimal colors). The second maximum disappears more and more and the curve becomes a smooth function of L^* for the absolute maximum $\Delta E_{ab,\max}$ (0%) at the colors of the L^* axis (neutral grey axis).

The results for $\Delta E^*_{94,\max}$ are shown in Figure 12 at the bottom. It is remarkable that only small differences between maximum color differences at the surface of the color gamut and at the center appear for this new color difference definition.

If the optimal color space given in tristimulus RGB components is quantized in such a manner that the maximum color quantization step $\Delta E_{ab,\max}$ is not larger than 1.0 throughout the color space for all lightness levels $L^* \geq 10$, then the following bit numbers are required (left-hand results).

Component	Range	Quantization Units (CIELAB-/CIE 94-formula)	Digitization for $\Delta E \approx 1$ (CIELAB-/CIE 94-formula)
R	$-41 \rightarrow 156$	0.0241/0.0483	13 bit/12 bit
G	$-15 \rightarrow 110$	0.0305/0.0305	12 bit/12 bit
B	$-12 \rightarrow 113$	0.0305/0.0611	12 bit/11 bit
		sum	37 bit/35 bit

The use of the new color difference definition and a threshold of $\Delta E^*_{94} \leq 1$ results in less effort (right-hand results).

4.3 Optimal Color Space Represented by Predistorted R′B′G′ Components and YCC Color Space

In view of the γ correction of cathode ray tubes, predistorted R′G′B′ signals are used in all systems with cathode ray displays. Predistorted R′G′B′ signals are also used in the YCC color space for storage of images on the Photo CD [Kodak 1992]. The definition follows the ITU-R BT.709 (formerly CCIR 709) recommendation with extended ranges of RGB components. In this article, the following definitions for predistortion have been assumed.

$$
\begin{aligned}
&R' = 1.099\ \mathrm{Sign}(R)|R|^{0.45} - 0.099;\ |R| \geq 0.018\\
&G' = 1.099\ \mathrm{Sign}(R)|G|^{0.45} - 0.099;\ |G| \geq 0.018\\
&B' = 1.099\ \mathrm{Sign}(R)|B|^{0.45} - 0.099;\ |B| \geq 0.018\\
&R' = 4.5\ R;\ G' = 4.5\ G;\ B' = 4.5\ B;\ |R|, |G|, |B| < 0.018.
\end{aligned}
$$

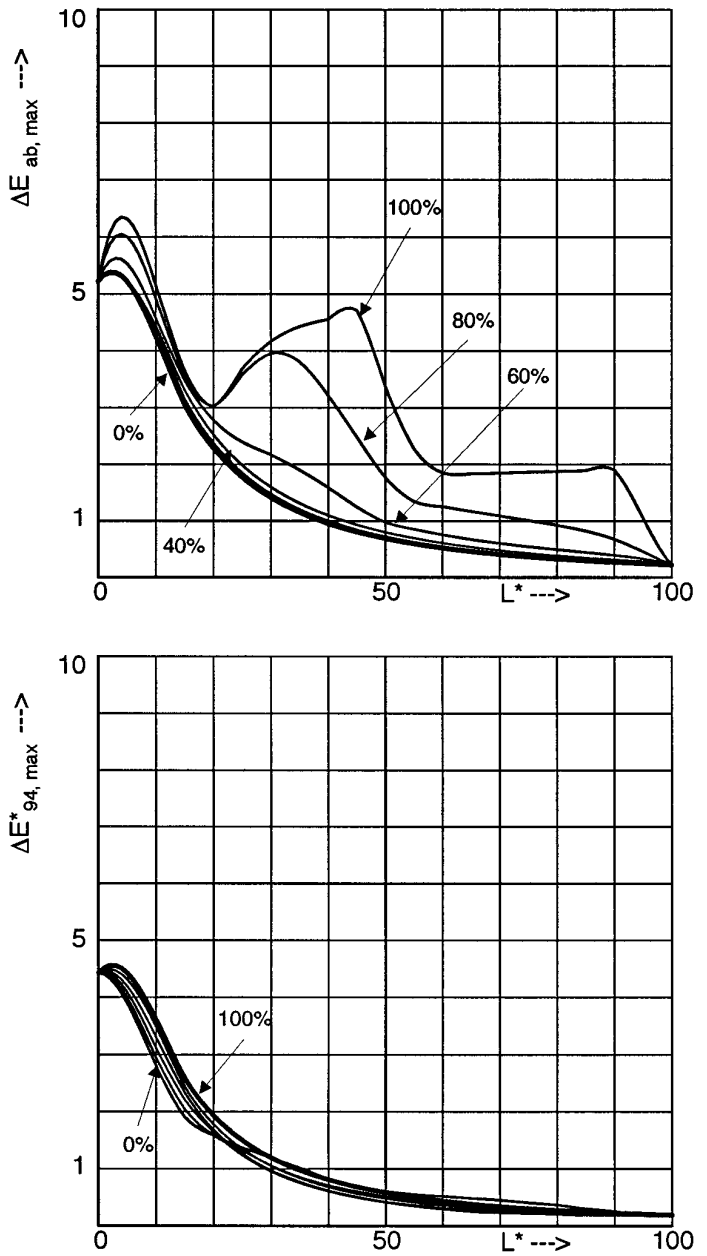

Fig. 12. Maximum color difference $\Delta E_{ab,\max}$ (top) and $\Delta E^*_{94,\max}$ (bottom) along lines of optimal colors (100%) in the quantized RGB space (10 bits per axis) at constant lightness L^* and lines with colors of reduced chroma given in % of the value of optimal colors vs. lightness level L^*.

The exponent of 0.45 corresponds to the γ value of 2.2. The optimal color space given by predistorted components has been studied in the same way as the optimal color space with tristimulus RGB components in the previ-

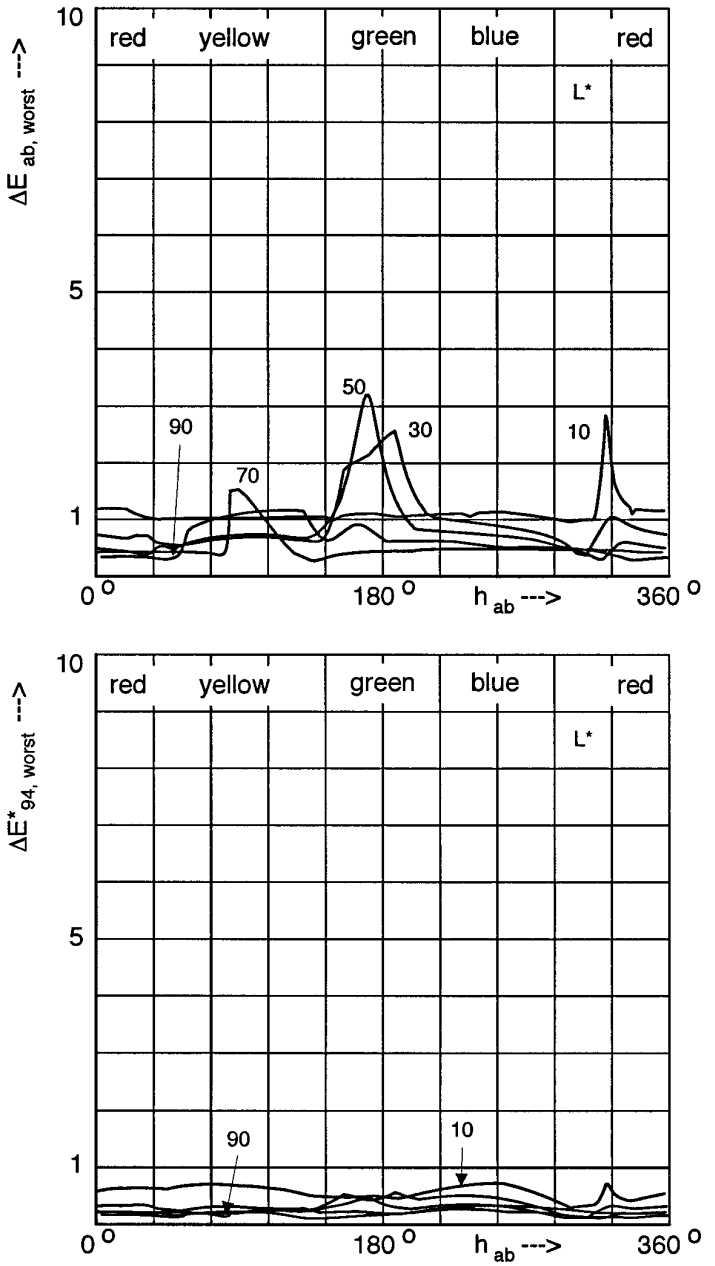

Fig. 13. Worst case color difference $\Delta E_{ab,\mathrm{worst}}$ (top) and $\Delta E^*_{94,\mathrm{worst}}$ (bottom) along lines of optimal colors at constant lightness L^* vs. hue angle for the quantization in the predistorted RGB space (10 bits per axis). Parameter: lightness L^* (Illuminant D65).

ous section. Figure 13 shows the $\Delta E_{ab,\mathrm{worst}}$ versus the hue angle h_{ab} for various lightness levels L^* resulting from the quantization of the optimal color space with predistorted R′G′B′ coordinates by 10 bits per component.

Again, the smallest possible quantization box just surrounding the space of optimal colors has been chosen. Compared to results for tristimulus RGB coordinates (Figure 11), the worst color quantization steps are shifted to lower values particularly at low lightness L^*. At high lightness, no dramatic changes appear. This is also demonstrated by the results in Figure 14 for the maximum color difference $\Delta E_{ab,\max}$ in planes of constant lightness at lines of optimal colors and lines of colors with reduced chroma. Compared to Figure 12, all curves are shifted to smaller values at low lightness L^*. Nevertheless, it is obvious that the quantization on the basis of predistorted R′B′G′ components does not result in greater uniformity of quantized color differences when assuming the CIE 1976 color difference formula.

This changes dramatically when the new CIE 94 formula is considered. The respective results for this formula are given at the bottom of Figures 13 and 14. For ΔE^*_{94} the peaks in the area of green colors at high chroma are reduced and the resulting color difference curves are not only located at lower levels, but are also more uniform.

If the optimal color space given in predistorted R′G′B′ components is quantized with the aim of keeping $\Delta E_{ab,\max[L^*\geq 10]} \leq 1$ or $\Delta E^*_{94,\max\ [L^*\geq 10]} < 1$, the following quantization concept of Table IV results.

Component	Range	Quantization Units (CIELAB-/CIE 94-formula)	Digitization for $\Delta E \approx 1$ (CIELAB-/CIE 94-formula)
R′	$-0.64 \rightarrow 1.25$	0.00046/0.00185	12 bit/10 bit
G′	$-0.37 \rightarrow 1.05$	0.00035/0.00139	12 bit/10 bit
B′	$-0.33 \rightarrow 1.06$	0.00034/0.00272	12 bit/9 bit
		sum	36 bit/29 bit

Compared to the results obtained for the tristimulus RGB coordinates, the win of only 1 bit for the ΔE_{ab} quantization is not effective. This is rooted in the peak value of $\Delta E_{ab,\max}$ at $L^* = 45$ on the surface of optimal colors (see Figures 12 and 14), which is not affected significantly by predistortion. For the quantization on the basis of ΔE^*_{94} the win is remarkable.

The YCC color space of Kodak [1992] is an interesting example of a predistorted color space, because it is used for the storage of color images on the Photo CD.

It is derived from the predistorted R′G′B′ coordinates given previously. Three components luma, chroma 1, and chroma 2 are defined by the following equations.

$$\begin{aligned} \text{luma} &= 0.299\ \text{R}' + 0.5876\ \text{G}' + 0.114\ \text{B}' \\ \text{chroma1} &= \text{B}' - \text{luma} \\ \text{chroma2} &= \text{R}' - \text{luma}. \end{aligned}$$

The coefficients of this equation follow the ITU-R BT.709 (formerly CCIR 709) recommendation. In Figure 15, the YCC color space is sketched within

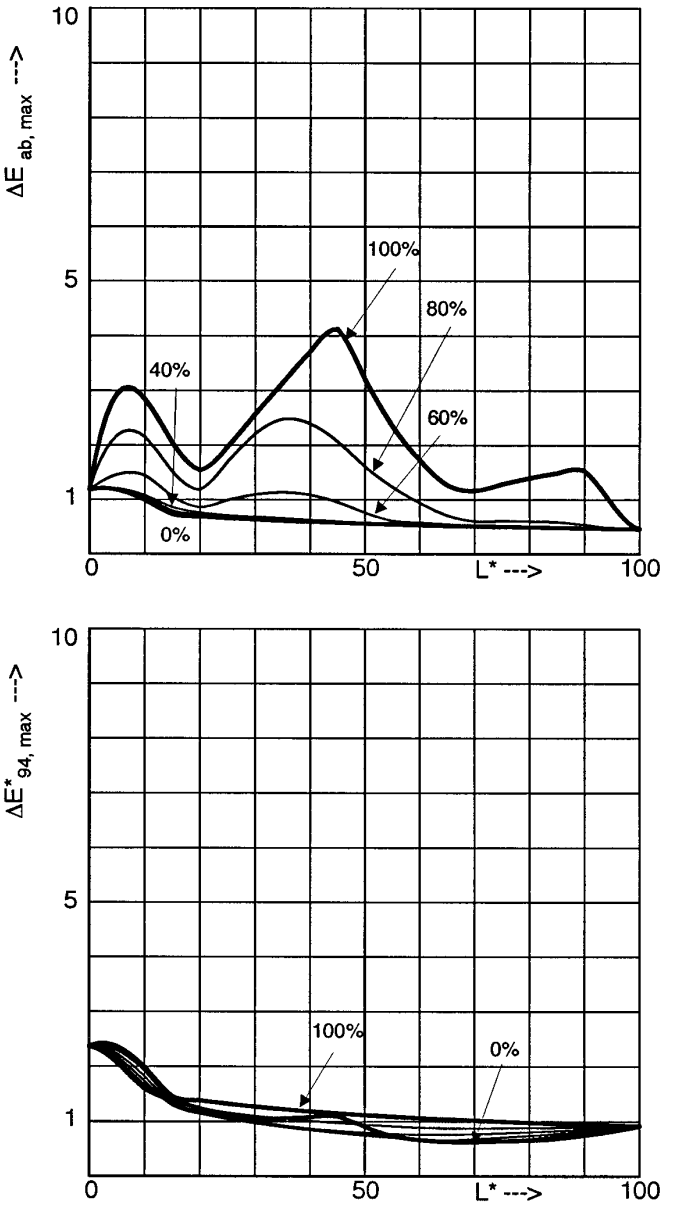

Fig. 14. Maximum color difference $\Delta E_{ab,\max}$ (top) and $\Delta E^*_{94,\max}$ (bottom) along lines of optimal colors (100%) in the predistorted and quantized R′G′B′ space (γ = 2.2 and 10 bits per axis) at constant lightness L^* and lines with colors of reduced chroma given in % of the value of optimal colors vs. lightness level L^*.

the limits of optimal colors transformed from the CIELAB optimal color space. The space is again composed of planes of constant lightness L^*; however, these planes become bowed due to predistortion. This gives the YCC color space a compact appearance.

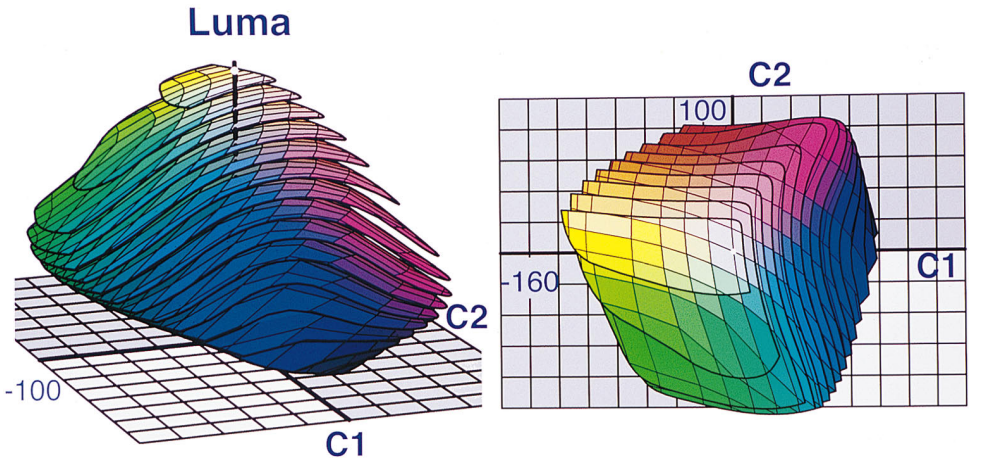

Fig. 15. Kodak YCC optimal color space composed of planes of constant L^* values with $\Delta L^* = 5$. The straight lines within each plane represent the lines of constant a^* values and lines of constant b^* values. On the right-hand side: top view on the YCC optimal color space. The uppermost plane corresponds to the lightness of $L^* = 95$. $L^* = 100$ gives the white point.

When looking from the top to the planes of constant lightness (right-hand side of Figure 15), the net of transformed a^*b^* lines in each plane appears quite uniform in a first view. Yet, at lower luma values, the net becomes very nonuniform. Therefore, the quantization of the YCC space delivers comparatively bad results.

The following study uses the quantization concept defined in Kodak [1992].

$$\begin{aligned} \text{luma}_{8\text{bit}} &= (255/1.402)\text{luma} \\ \text{chroma1}_{8\text{bit}} &= 11.40\ \text{chroma1} + 156 \\ \text{chroma2}_{8\text{bit}} &= 135.64\ \text{chroma2} + 137. \end{aligned}$$

If the optimal colors are represented by this concept, the ranges of the coordinates are to be considered:

$$\begin{aligned} 0 \le \text{luma} \le 1.0 \quad &; \quad 0 \le \text{luma}_{8\text{bit}} \le 182 \\ -1.169 \le \text{chroma1} \le 0.987 \quad &; \quad 25 \le \text{chroma1}_{8\text{bit}} \le 266 \\ -1.043 \le \text{chroma2} \le 0.885 \quad &; \quad -5 \le \text{chroma2}_{8\text{bit}} \le 253. \end{aligned}$$

Hence, the limited range of the 8-bit quantization (0 to 255) is slightly overmodulated by the optimal colors considered. The colors assumed originally for the Photo CD cover a smaller space. Yet the range of colors overmodulating the system is small and the following results do not change remarkably when clipping the colors to the digital values of 255 or 0.

In Figure 16 (top), the worst color quantization steps $\Delta E_{ab,\text{worst}}$ versus hue angle are given for the 8-bit quantization of the optimal colors in the YCC space and in Figure 17 (top), the respective maximum values $\Delta E_{ab,\text{max}}$

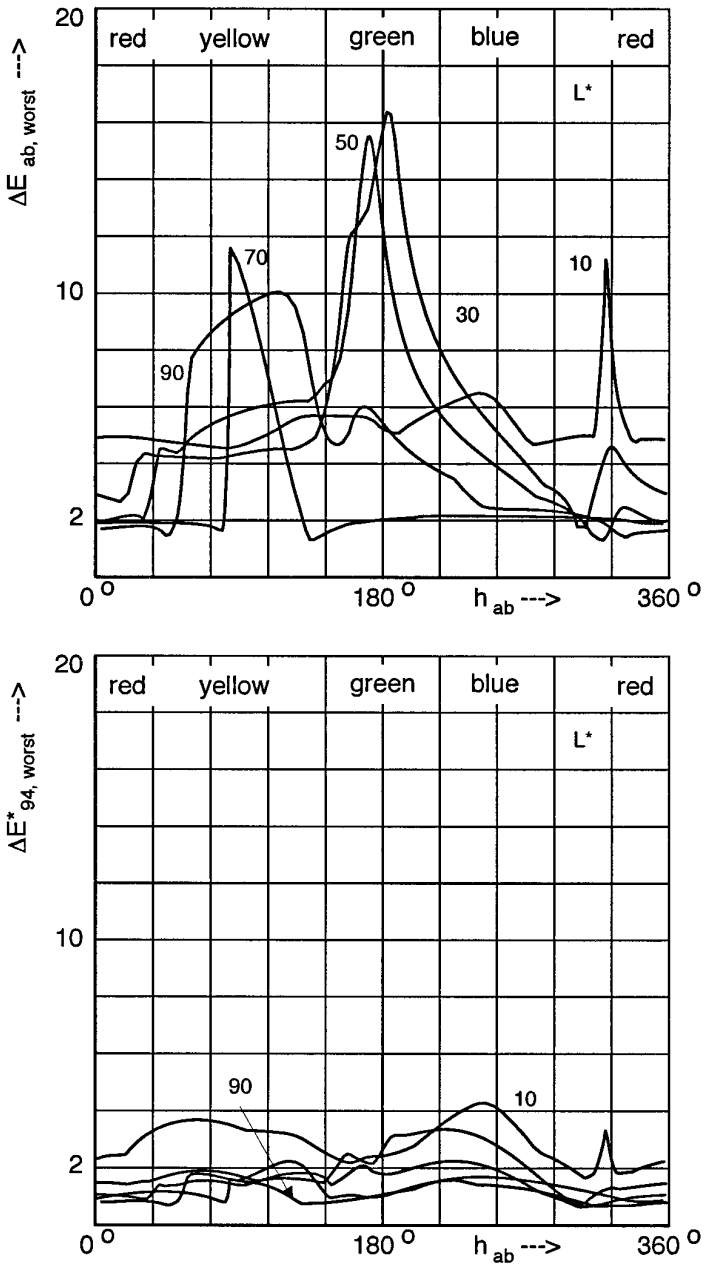

Fig. 16. Worst case color difference $\Delta E_{ab,\text{worst}}$ (top) and $\Delta E^*_{94,\text{worst}}$ (bottom) along lines of optimal colors at constant lightness L^* vs. hue angle for the quantization in the Kodak YCC space (8 bits per axis). Parameter: lightness L^* (Illuminant D65).

versus lightness L^* are plotted. It turns out that large color differences for the worst steps in the grid of quantized colors appear. Even when the colors are restricted to chroma values of 80% of the values of optimal colors at the

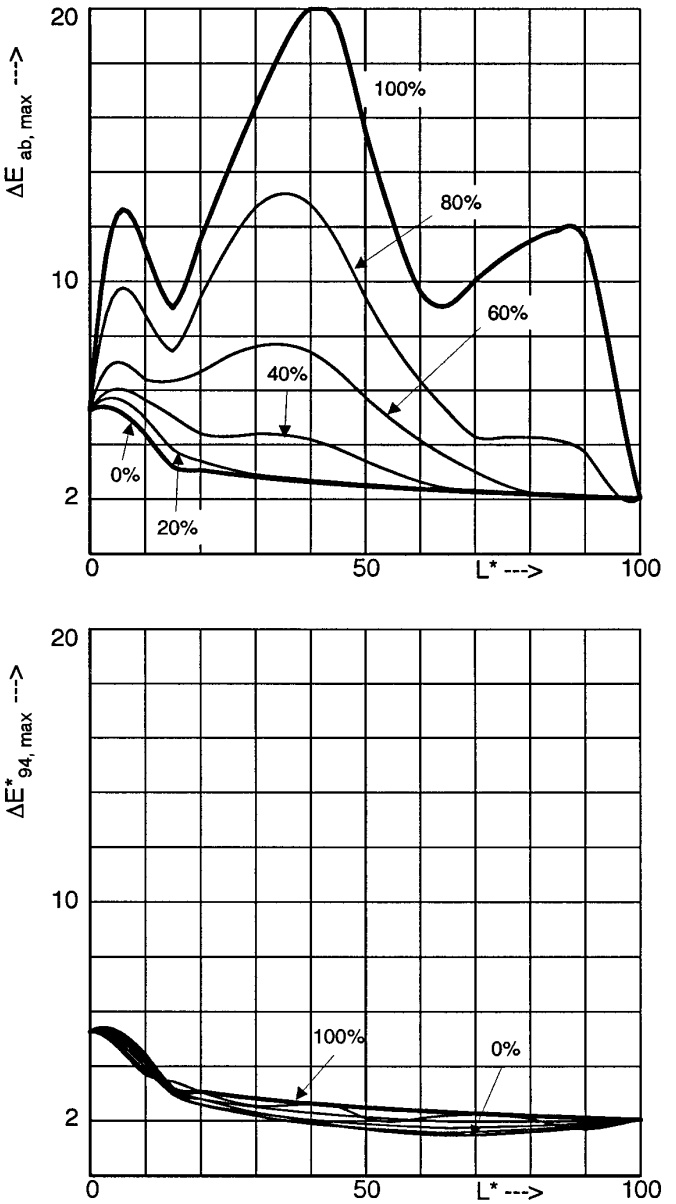

Fig. 17. Maximum color difference $\Delta E_{ab,\max}$ (top) and $\Delta E^*_{94,\max}$ (bottom) along lines of optimal colors (100%) in the predistorted and quantized Kodak YCC color space (8-bit per axis) at constant lightness L^* and lines with colors of reduced chroma given in % of the value of optimal colors, versus lightness level L^* (Illuminant D65).

same hue angle (80% curve in Figure 17), peak values of up to 13 are found. Compared with the results of the predistorted R′G′B′ space (Figure 14), the peak values of Figure 17 (top) are larger by a factor of more than 4. The factor 4 is understandable from different quantization of 10 + 10 + 10 bits

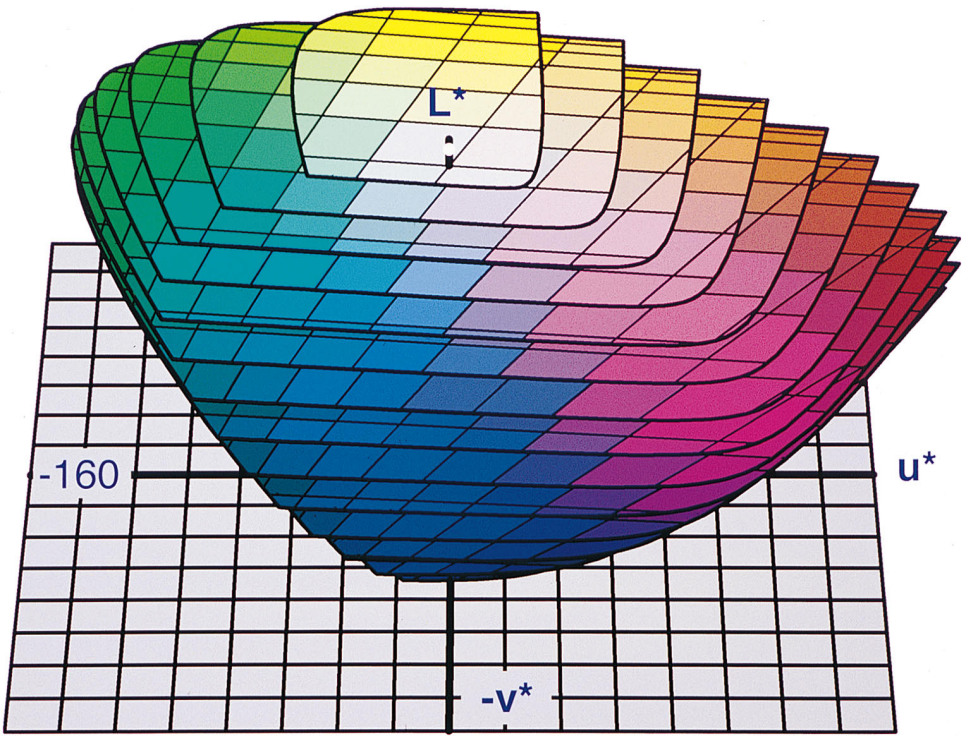

Fig. 18. CIELUV optimal color space with planes of constant lightness L^* arranged 5 units one upon the other and the net of a^*-, b^*-lines 20 ΔE_{ab} units apart within each plane.

compared to 8 + 8 + 8 bits but, in addition, the optimal colors use only 65% of the complete range of 256 digital steps in the quantization concept given in Kodak [1992].

The valuation of the color distances by the new CIE 94 formula at the bottom of Figures 18 and 19 leads to remarkably smaller worst-case values. All the values of $\Delta E^*_{94,\mathrm{worst}}$ (Figure 18) lie below 4.5 and the maximum values $\Delta E^*_{94,\mathrm{max}}$ as a function of lightness L^* (Figure 19) within the color space are all concentrated within a range of 2 to 5.

5. COMPARISON TO THE CIELUV OPTIMAL COLOR SPACE

The CIELUV space proposed as an alternative approximately uniform color space uses instead of the a^*- and b^*-coordinates the coordinates u^* and v^*, that are certain projections of the x- and y-coordinates of the CIE xy chromaticity diagram [CIE 1986b].

The total color difference is defined by

$$\Delta E_{uv} = \sqrt{\Delta L^{*^2} + \Delta u^{*^2} + \Delta v^{*^2}}.$$

Using these definitions, the optimal color space of Figure 2 has been transformed via the XYZ system into L^*-, u^*-, v^*-coordinates. Figure 18

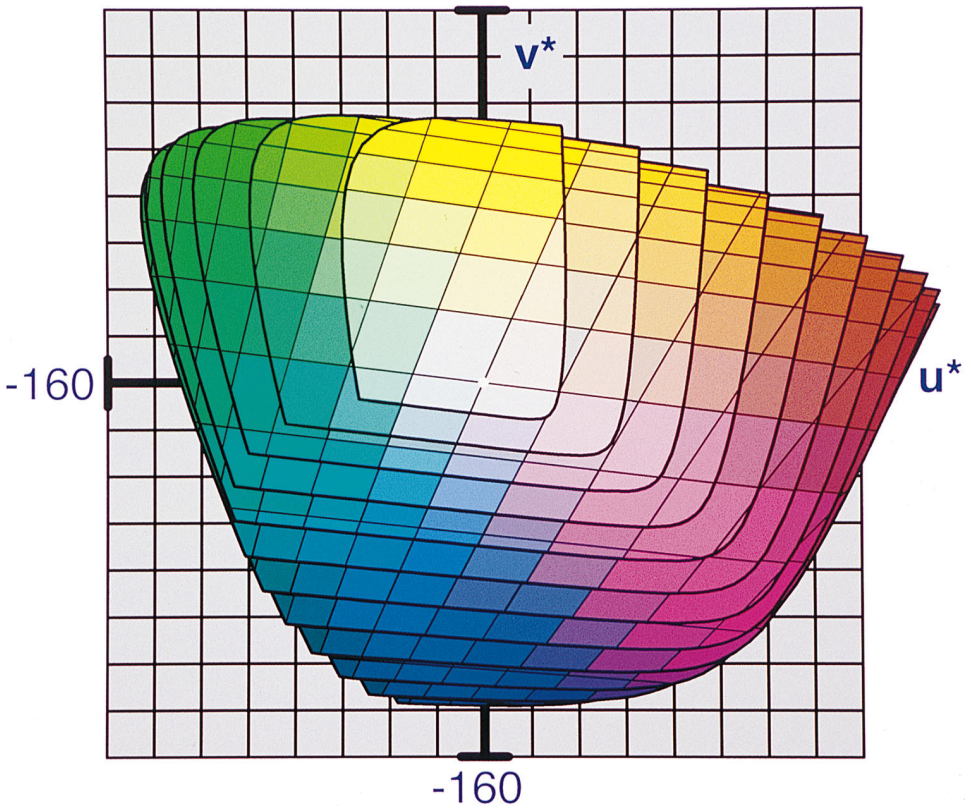

Fig. 19. Top view on the CIELUV optimal color space.

shows a side view and Figure 19 a top view of the resulting CIELUV optimal color space. For values of Y/Yn above a threshold of 0.1, the lightness L^* uses the same definition as the CIELAB system. The equidistant planes of the CIELAB space are consequently imaged into equidistant planes in the CIELUV space. The top view of Figure 19, on the other hand, demonstrates essential differences between the rectangles of the a^*- and b^*-net in the CIELAB space (Figure 3) and their projections into the CIELUV space within each plane of $L^* = \text{const.}$

The lines $a^* = \text{const.}$ and $b^* = \text{const.}$ are again projected into straight lines, but they are arranged at certain angles to the u^* and v^* axes. Therefore all the hue values are twisted clockwise compared to the CIELAB space. The lines $a^* = \text{const.}$ (blue to yellow) are twisted more than the lines $b^* = \text{const.}$ (green to red) and, in addition, the angle of twisting increases with u^* and v^*; therefore each square with $\Delta a^* = \Delta b^* = 20$ units of the CIELAB space is transformed into a distorted quadrangle in the CIELUV space.

Near the grey axis L^* and in the complete range of blue and red, the size of these quadrangles (20 $a^* \times 20$ b^* units) appears enlarged. This means that color is represented as more compressed in this range of the CIELAB

space compared to the CIELUV space. On the other hand, the quadrangles are compressed and condensed near the optimal color border of yellow and green colors, an effect which grows with the distance from the L^* axis. The dark "colors of the blue" giving the CIELAB space its typical "nose" are projected into compressed areas in the CIELUV space and twisted clockwise with respect to the u^*- and v^*-axes, resulting in a "more compact" shape of the CIELUV space.

The volume of the CIELUV optimal color space in terms of L^*, u^*, v^* coordinates results in $2.770 \cdot 10^6$. It is almost 1.37 times "larger" than the volume of the CIELAB optimal color space expressed in CIELAB units. The number of distinguishable colors resulting from the model of highest ball density results in $3.915 \cdot 10^6$. Thus the CIELUV space defines about 20% more colors than the CIELAB space.

The largest dimensions of the CIELUV optimal color space in terms of L^*, u^*, and v^* coordinates are of the same order as those of the CIELAB space in terms of L^*, a^* and b^* coordinates: $0 \le L^* \le 100$, $-145 \le u^* \le 193$; $-138 \le v^* \le 115$.

If the CIELUV color difference formula is applied to the quantization of the CIELUV optimal color space and the value $\Delta E_{uv} \approx 1$ is considered as an approximate limit to color distinction, the quantization concept is:

Component	Range	Quantization Units	Digitization for $\Delta E \approx 1$
u^*	$-145 \rightarrow 193$	0.6614	9 bit
v^*	$-138 \rightarrow 115$	0.4941/0.9883	9 bit/8 bit
L^*	$0 \rightarrow 100$	0.3906/0.7813	8 bit/7 bit
		sum	26 bit/24 bit

Thus quantization of the CIELUV optimal color space in terms of ΔE_{uv} requires the same effort as that of the CIELAB optimal color space in terms of ΔE_{ab}.

Essential differences between the definitions of color differences in the CIELUV and the CIELAB space appear if the CIELUV space is digitized according to the preceding concept, but if the resulting color differences in the quantization cells are valued by the CIELAB color difference formula.

In Figure 20, the worst color quantization steps $\Delta E_{ab,\text{worst}}$ have been plotted against the hue angle h_{ab} for the borderlines of optimal colors of the CIELUV space quantized into $L^*u^*v^* \rightarrow 8 + 9 + 9$ bits and for the respective quantized grid of points transformed into CIELAB coordinates. Very high values of $\Delta E_{ab,\text{worst}}$ appear in the range where the CIELAB space shows its "blue nose." Such a nose is completely suppressed in the CIELUV space.

A second range, where large color differences between quantized grid points appear, is the range of yellow to green colors at high lightness. Both ranges demonstrate the largest differences between both color spaces. In Figure 21, the maximum color quantization steps $\Delta E_{ab,\max}$ between grid

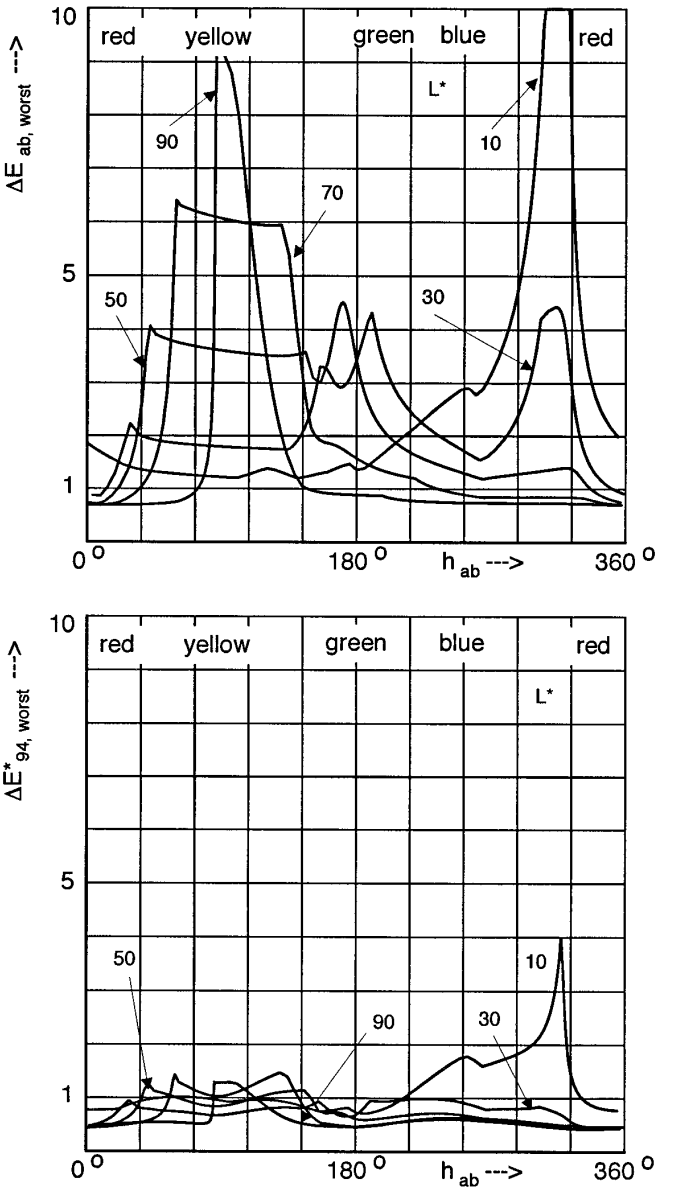

Fig. 20. Worst case color difference $\Delta E_{ab,\mathrm{worst}}$ (top) and $\Delta E^*_{94,\mathrm{worst}}$ (bottom) vs. hue angle for the digitization of the CIELUV space into L^*, u^*, $v^* \rightarrow 8 + 9 + 9$ bit and valuation of the respective quantization cells by the CIELAB color difference formula. The 5 curves represent the maximum color differences per quantization cell along the border of optimal colors in planes of constant lightness $L^* = 10$, 30, 50, 70, and 90.

points along the borderlines of optimal colors (100%) and along lines with reduced chroma are plotted versus the lightness L^*. The 0% curve gives the $\Delta E_{ab,\mathrm{max}}$ values along the grey axis. Again, there is little consistency between the valuation of color differences in the CIELAB space and the

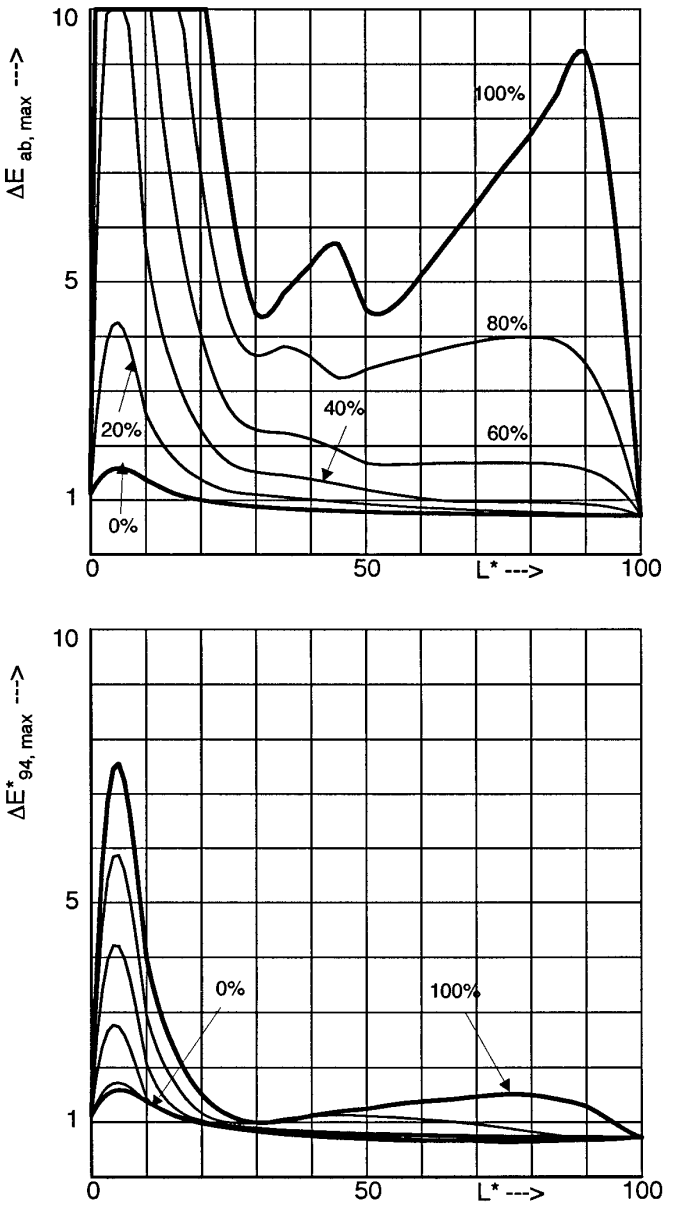

Fig. 21. Maximum color difference $\Delta E_{ab,\max}$ (top) and $\Delta E^*_{94,\max}$ (bottom) along lines of optimal colors (100%) in the quantized CIELUV color space (8 + 9 + 9 bits per axis) expressed in CIELAB coordinates at constant lightness L^* and lines with colors of reduced chroma given in % of the value of optimal colors vs. lightness level L^*.

CIELUV space demonstrated. Only at high lightness and for the inner part of the color spaces around the grey axis does the valuation of color differences in both spaces come to similar results ($\Delta E_{ab,\max} = \Delta E_{uv,\max} = 1$).

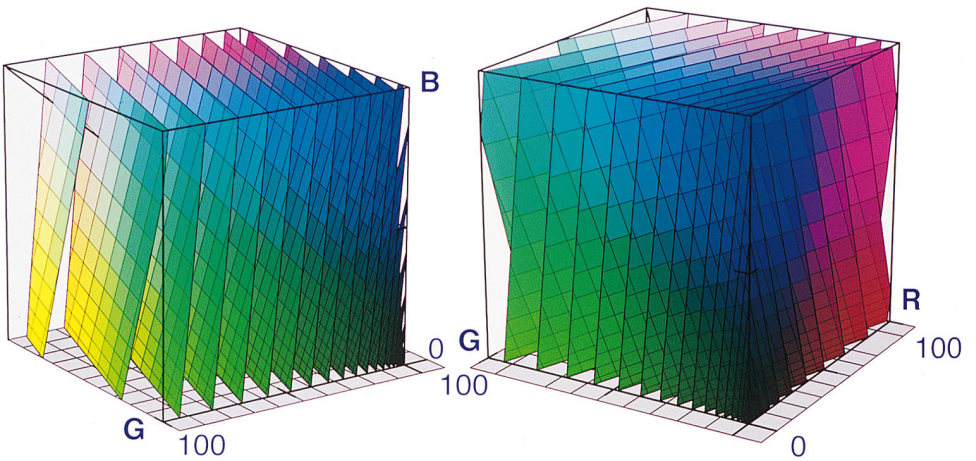

Fig. 22. Positive RGB cube. Inside the RGB cube, planes of constant lightness L^* are arranged (see Figure 2). The net indicated in each plane represents lines of constant a^* or b^* with the line spacings of 20 units. The diagonal from the zero point to R = G = B = 100 represents the gray axis.

The results on the basis of the CIELAB 94 color difference formula (bottom of Figures 20 and 21) show much more consistency. The valuation of the CIELUV space with the CIELAB 94 formula leads to values of $\Delta E^*_{94,\text{worst}}$ around one in nearly all parts of the color space save in the range of the "blue nose" of the CIELAB space of low lightness. This is confirmed by the plot of $\Delta E^*_{94,\text{max}}$ in Figure 21 (bottom). Obviously, the new color difference formula CIELAB 94 matches the CIELUV color difference formula quite well with the exception of the range of low lightness $L^* < 15$.

6. DEVICE DEPENDENT COLOR SPACES

6.1 The Positive RGB Cube

The tristimulus RGB color space is defined by three chromaticity coordinates derived from the primary colors of three phosphors of a cathode ray tube. Therefore practical RGB signals for additive color mixing cover only the positive range. In addition, the components are referenced to a white illuminant D65 and white values are assumed for R = G = B = 100. The color space of the linear RGB system therefore forms a simple cube with coordinates between 0 and 100 (called a positive RGB cube in the following). Two views of a linear RGB cube following the ITU-R BT.709 (formerly CCIR 709) definition are shown in Figure 22. Within the cubes, planes of constant lightness L^* transformed from the CIELAB space into the cube are shown together with the net of a^*b^* lines spaced 20 units apart. The transformation of the positive RGB cube into CIELAB coordinates is shown in Figure 23. From this representation, the number of perceivable colors of

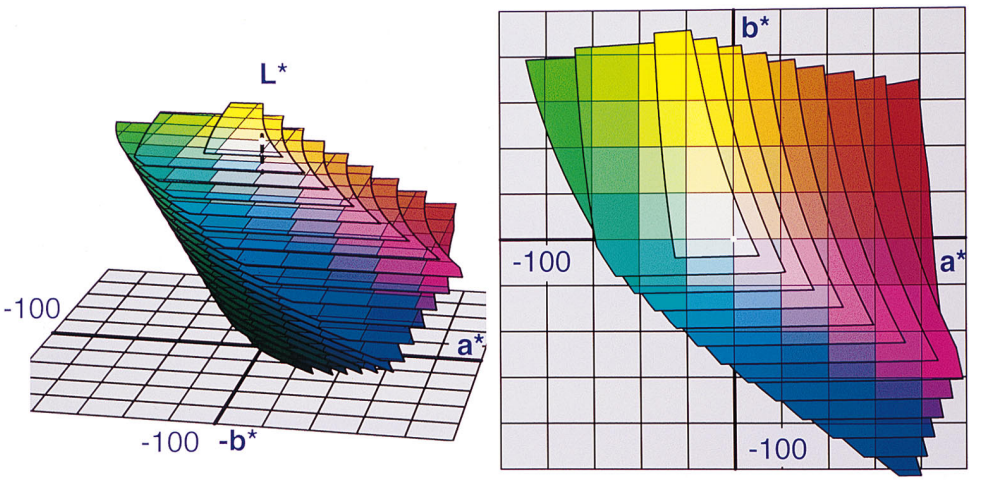

Fig. 23. CIELAB color space within the limits of positive RGB components. The planes of constant lightness L^* are spaced $\Delta L^* = 5$ (left). Top view on the CIELAB color space within the limits of RGB_{EBU} components. The values of maximum dimensions in the a^*-, b^*-plane are $a^*_{min} = -88$, $a^*_{max} = 98$, $b^*_{min} = -103$, and $b^*_{max} = 91$ (right).

the positive RGB cube can be estimated using the assumptions from Section 3.

The model of highest ball density with balls of the diameter of $\Delta E_{ab} = 1$ deliver $1.18 \cdot 10^6$ colors. This is about one-third of the number of colors represented by the optimal color space.

In most practical applications, the components of the positive RGB cube are digitized into 8 + 8 + 8 bits. For this concept, the grid of quantized points of the cube has been transformed into CIELAB coordinates and the maximum color quantization steps between neighboring points of the grid in each plane of constant lightness L^* have been calculated. $\Delta E_{ab,max}$ vs. L^* is plotted in Figure 24 for grid points along the surface of the color space (100% line) and for grid points on surfaces with reduced chroma with respect to the chroma values at the outer surface with the same hue angle and lightness. The absolute peak value (clipped in Figure 24) is found to be 12.8 at $L^* = 5$.

The quantization of the positive RGB cube into a grid which keeps the maximum $\Delta E_{ab,max}$ or $\Delta E^*_{94,max}$ below a value of 1 for all lightness values $L^* > 10$ results in the following:

Component	Range	Quantization Units (CIELAB-/CIE 94-formula)	Digitization for $\Delta E \approx 1$ (CIELAB-/CIE 94-formula)
R	$0 \rightarrow 100$	0.0489/0.0489	11 bit/11 bit
G	$0 \rightarrow 100$	0.0244/0.0244	12 bit/12 bit
B	$0 \rightarrow 100$	0.0244/0.0489	12 bit/11 bit
		sum	35 bit/34 bit

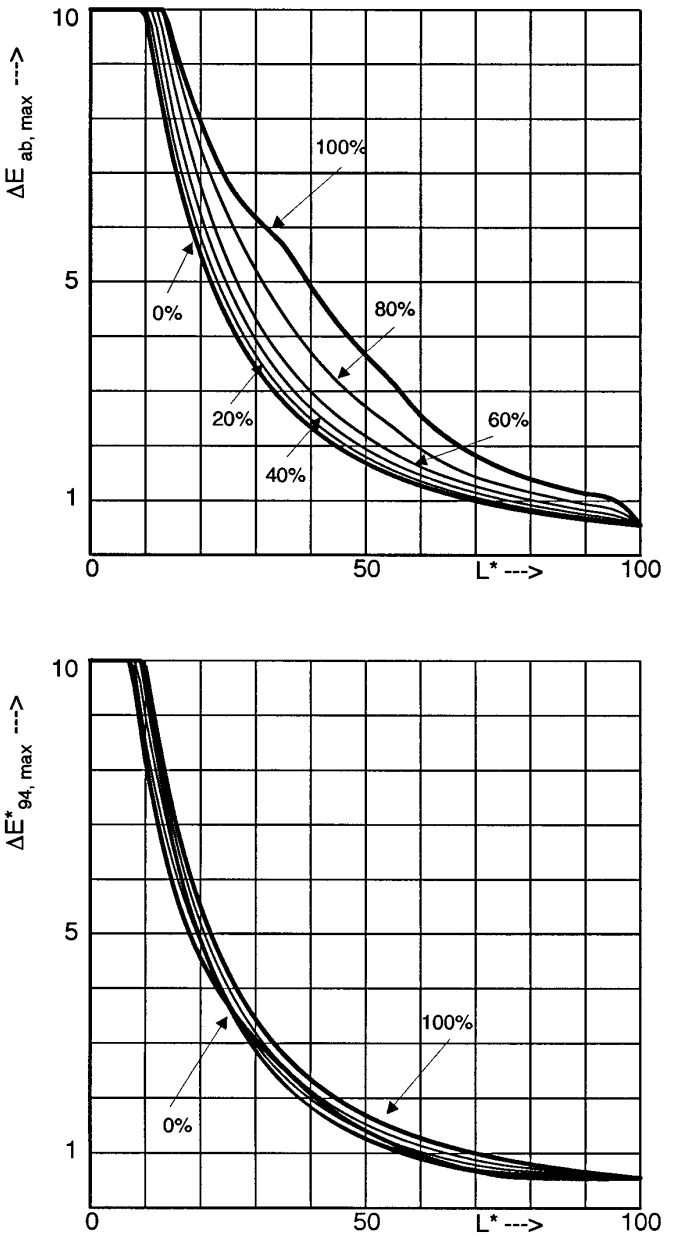

Fig. 24. Maximum color difference $\Delta E_{ab,\max}$ (top) and $\Delta E^*_{94,\max}$ (bottom) for the digitization of the positive RGB cube (8 + 8 + 8 bit) along the border in the plane of given lightness. 0%: test points along the grey axis. Other: test points along lines "parallel" to the borderline at reduced chroma given in percent.

If the positive RGB cube transformed into CIELAB coordinates as shown in Figure 23 is quantized, the results will be much better and 8 + 8 + 8 bit are sufficient:

Component	Range	Quantization Units	Digitization for $\Delta E \approx 1$
a^*	$-88 \rightarrow 98$	0,7294	8 bit
b^*	$-103 \rightarrow 91$	0,7608	8 bit
L^*	$0 \rightarrow 100$	0,3922	8 bit
		sum	24 bit

6.2 Predistorted Positive R′G′B′ Cube (ITU-R BT.709)

As most of the electrical signals for controlling displays use predistorted R′G′B′ components, results for the quantization of a predistorted R′G′B′ color space with $\gamma = 2.2$ are given in Table VIII. Curves $\Delta E_{ab,\max}$ versus L^* for this case are given in Figure 25. As outlined in Section 4.3, predistortion reduces the color steps due to quantization in the range of low lightness. It is obvious from Figure 25 that predistortion within the limits of a positive RGB cube delivers a remarkable improvement of $\Delta E_{ab,\max}$ compared to Figure 24. This looks even better if the calculation is based on ΔE^*_{94} (Figure 25, bottom). Accordingly, the quantization under the condition of $\Delta E_{ab,\max} \leq 1$ leads to a win of 7 bits compared to the quantization of the positive RGB cube using undistorted tristimulus RGB components.

Component	Range	Quantization Units (CIELAB-/CIE 94-formula)	Digitization for $\Delta E \approx 1$ (CIELAB-/CIE 94-formula)
R′	$0 \rightarrow 1$	0.00196/0.00196	9 bit/9 bit
G′	$0 \rightarrow 1$	0.00196/0.00196	9 bit/9 bit
B′	$0 \rightarrow 1$	0.00098/0.00196	10 bit/9 bit
		sum	28 bit/27 bit

For comparison, the YCC color space as described in Section 4.3 and defined in Kodak [1992] has been analyzed as well for the range of input components within the positive RGB cube. The maximum color quantization steps $\Delta E_{ab,\max}$ vs. L^* are shown in Figure 26. Peak color quantization steps of up to 5.8 do appear. However, they lie in a range $L^* < 20$ and are much smaller than the peak errors in the YCC space limited by optimal colors. The curves $\Delta E^*_{94,\max[L^* \geq 10]} \leq 1$ have a different distribution along L^* in this case, although the amplitudes are nearly the same.

6.3 Color Spaces of Technical Print Processes

6.3.1 *Thermal Dye Sublimation Printer.* One of the most successful technologies in the electronic printing of full color images is that of the thermal dye sublimation printer. The color space of the Mitsubishi S3600-30 sublimation printer has been analyzed and the gamut of colors has been derived by printing a selected number of test colors and determining the respective tristimulus values by accurate spectral measurement equipment. An optimized three-dimensional transformation and interpolation algorithm has been developed to determine intermediate color values and to describe the surface of the resulting color space. The graphical

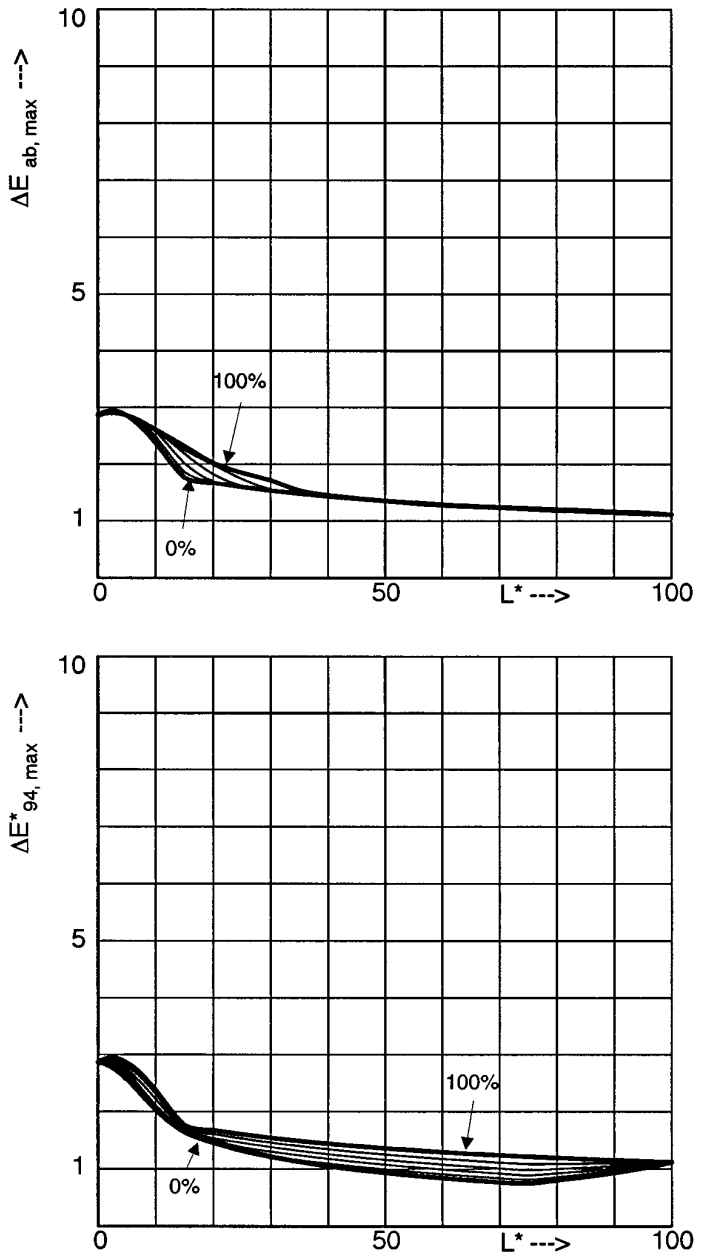

Fig. 25. Maximum color quantization steps $\Delta E_{ab,\max}$ (top) and $\Delta E^*_{94,\max}$ (bottom) vs. lightness L^* for the digitization of the predistorted R′G′B′ color space (8 + 8 + 8 bit). 100%: test points along the border in the plane of given lightness. 0%: test points along the grey axis. Other: test points along lines "parallel" to the borderline at reduced chroma given in percent.

presentations in Figure 27 are again composed of the planes of constant lightness L^*. The color gamut has been derived for the printer option with only three printing colors (CMY).

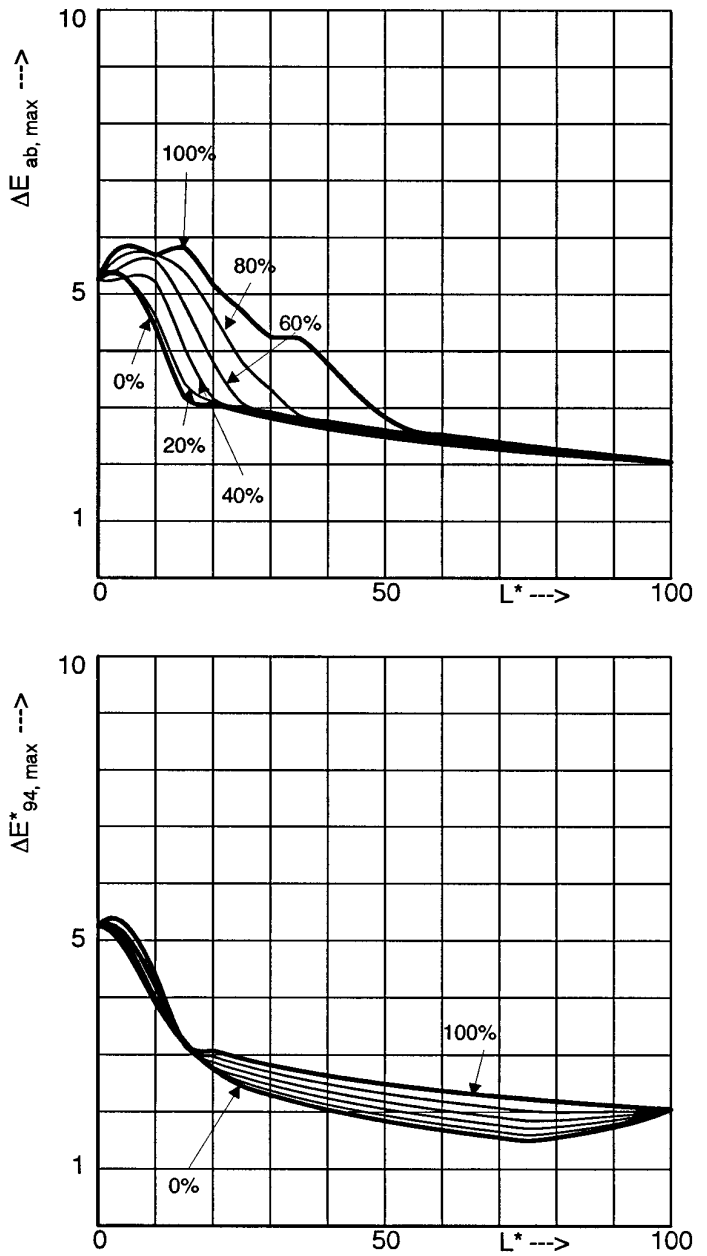

Fig. 26. Maximum color quantization steps $\Delta E_{ab,\max}$ (top) and $\Delta E^*_{94,\max}$ (bottom) vs. lightness L^* for the digitization of the YCC space (8 + 8 + 8 bit) assuming positive RGB components only. 100%: test points along the plane of given lightness. 0%: test points along the grey axis. Other: test points along lines "parallel" to the borderline at reduced chroma given in percent.

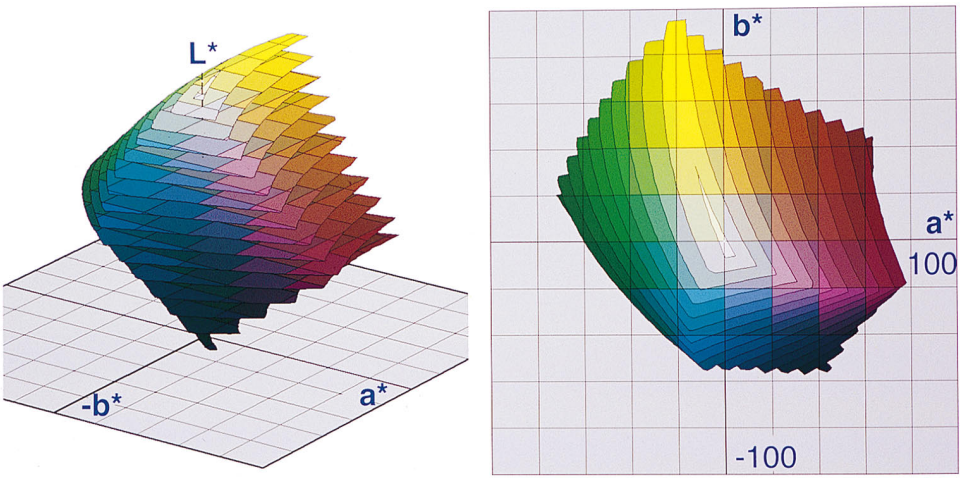

Fig. 27. CIELAB color space of the Mitsubishi S3600-30 thermal dye sublimation printer. The planes of constant lightness L^* are spaced $\Delta L^* = 5$ (left). Top view on the CIELAB color space within the limits of CMY printing dye values between 0% and 100%. The values of maximum dimensions in the a^*-, b^*-plane are $a^*_{\min} = -72$, $a^*_{\max} = 78$, $b^*_{\min} = -58$, and $b^*_{\max} = 95$ (right).

For device-independent color description, it is necessary to reference the measured tristimulus values of a printed test sheet to an absolute standard. Therefore the value of $L^* = 0$ has been attached to absolutely black and $L^* = 100$ to white (barium sulfate white standard) for the illuminant D65. Within this scale, the printer does not reproduce values below $L^* = 18$ and above $L^* = 95$ with three colorants. The white point of the paper is found at $L^* = 95$.

The number of colors resulting from the model of highest ball density is $0.627 \cdot 10^6$. In this case, about 50% of the colors of the RGB space are included. However, the RGB color space does not surround the color space of the sublimation printer completely. In the range of dark colors, there are areas where the colors of the thermal dye sublimation printer lie outside the RGB color space.

In Figure 28, the plane $L^* = 50$ of the color space of a thermal dye sublimation printer has been plotted together with the border lines of the RGB space and the optimal color space.

There is a large area of colors in the range of saturated blue and green colors that can be reproduced by the thermal dye sublimation printer but not by the positive components of RGB. On the other hand, a large part of colors of the RGB space cannot be reproduced by the printer. If an electronic image to be printed contains those colors, they must be replaced by other printable colors using gamut mapping.

The quantization is required to describe the full range of reproducible colors of the dye sublimation printer in the CIELAB space.

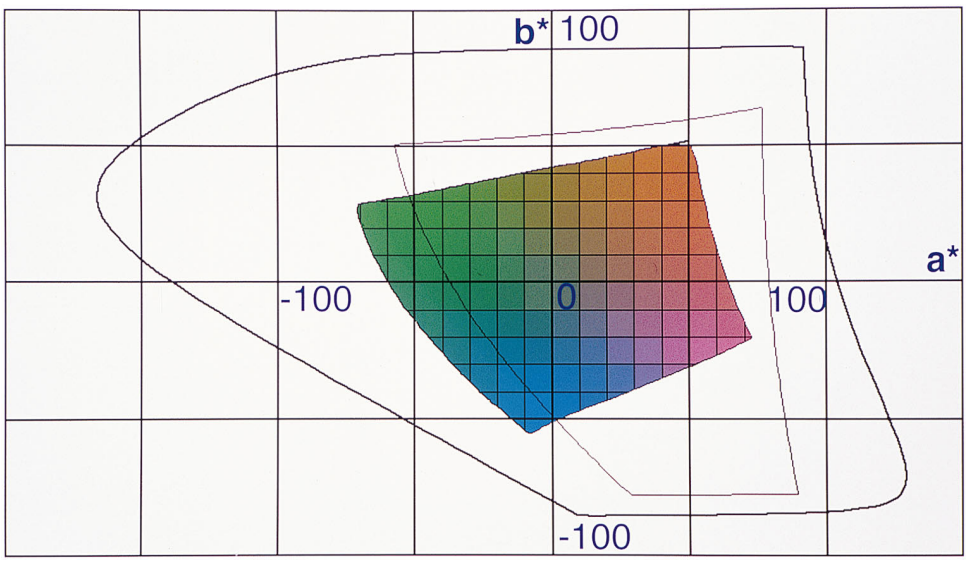

Fig. 28. Plane $L^* = 50$ of the color space of thermal dye sublimation printer (colored) and border lines of the positive RGB cube (thin line) and the optimal color space (thick line).

Component	Range	Quantization Units	Digitization for $\Delta E \approx 1$
a^*	$-72 \rightarrow 78$	0,5882	8 bit
b^*	$-58 \rightarrow 95$	0,6000	8 bit
L^*	$18 \rightarrow 95$	0,6063	7 bit
		sum	23 bit

Control of the printer by CIELAB values of 8 + 8 + 7 bits is accordingly the most effective way to represent all the printable colors. If, however, the printer is controlled by RGB signals, the following quantization would be required under the assumptions of keeping $\Delta E_{ab,\max[L^* \geq 10]} \leq 1$ or $\Delta E^*_{94,\max[L^* \geq 10]} \leq 1$. No improvement is achieved on the basis of the CIE 94 formula in this case.

Component	Range	Quantization Units (CIELAB-/CIE 94-formula)	Digitization for $\Delta E \approx 1$ (CIELAB-/CIE 94-formula)
R	$-9 \rightarrow 103$	0,1095/0,1095	10 bit/10 bit
G	$0 \rightarrow 104$	0,0508/0,0508	11 bit/11 bit
B	$-2 \rightarrow 112$	0,1114/0,1114	10 bit/10 bit
		sum	31 bit/31 bit

6.3.2 *Cromalin and Match Print Proofing Systems.* The Cromalin and Match Print processes are often used for proofing purposes in professional printing. Figure 29 shows both color spaces in CIELAB coordinates.

The number of printable colors estimated from the model of highest ball density results in $0.484 \cdot 10^6$ for the Cromalin process and in $0.455 \cdot 10^6$ for Match Print. Hence the number of printable colors is of the same order for

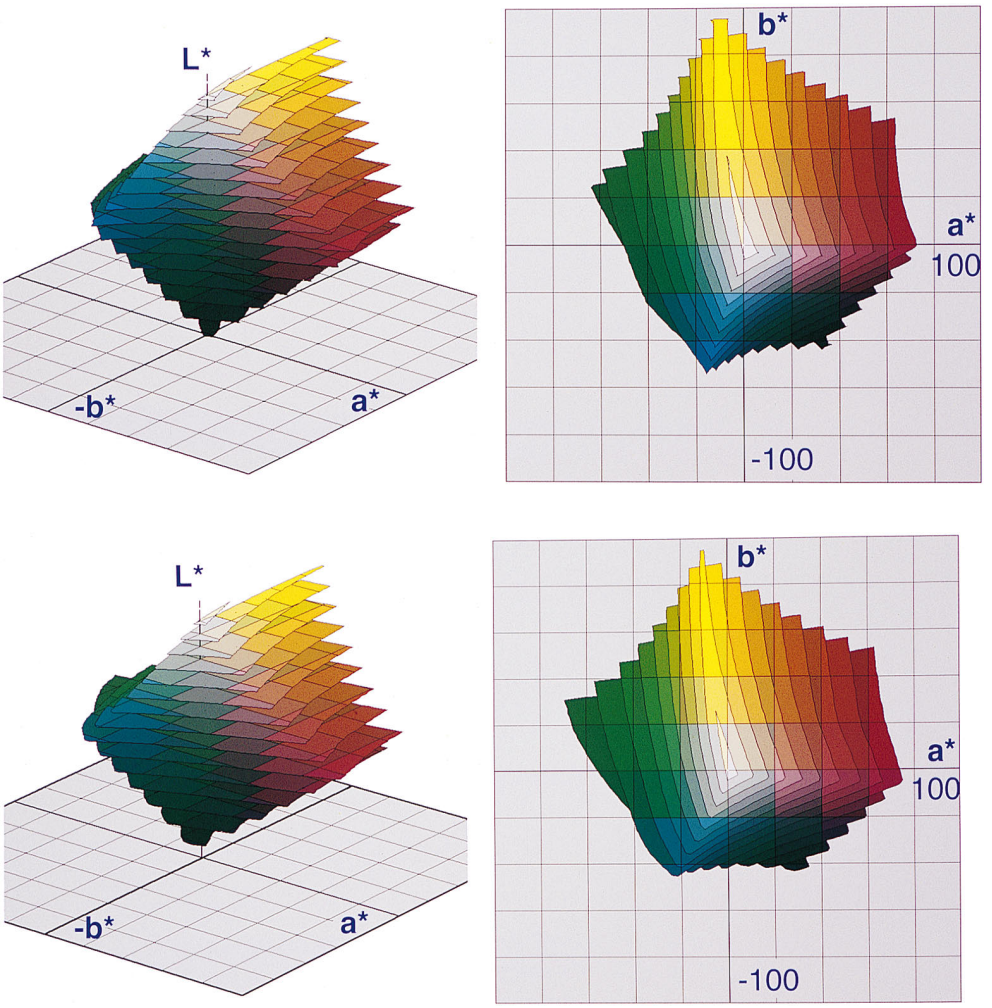

Fig. 29. Cromalin (upper) and Match Print (lower) color spaces given in CIELAB coordinates.

both printers, although there are some differences in detail. More colors are reproduced by the Cromalin process in the blue range, whereas Match Print reproduces a few more green colors. It is also obvious that the color space of the thermal dye sublimation printer occupies a larger range of colors than the conventional proofing systems considered (see Figures 27 and 29). This fact is also demonstrated by the planes of constant lightness $L^* = 50$ in Figure 30 compared to Figure 28.

Only a small part of the colors of the RGB space is occupied by the respective gamuts of the print process. This points to the difficulty when comparing images displayed on a cathode ray tube with prints. A good correspondence will only be achieved if the display is controlled via a color processor that reduces the colors of an electronic image to the gamut of the printer using the same gamut mapping as applied to the print process.

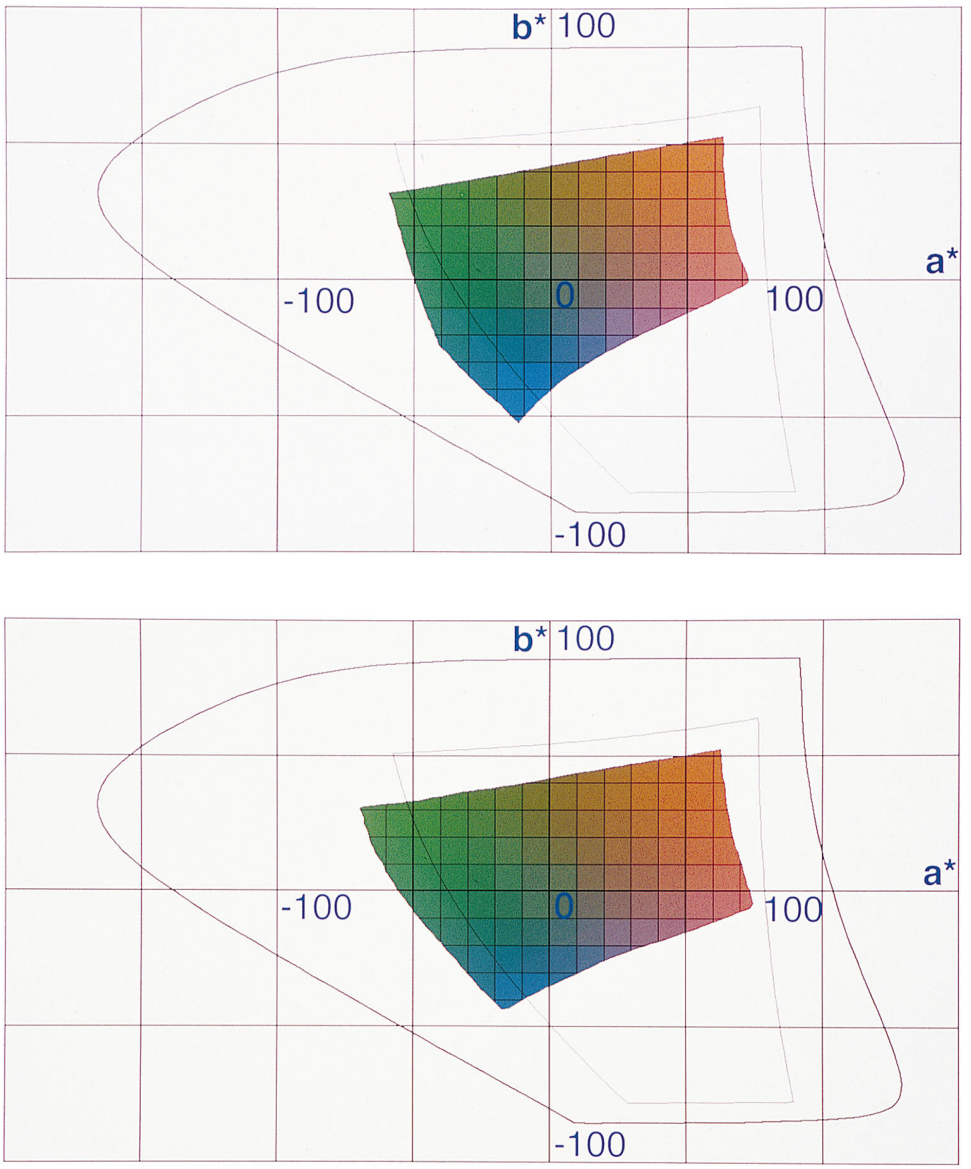

Fig. 30. Planes of constant lightness $L^* = 50$ of the Cromalin (upper) and Match Print (lower). The positive RGB limit is given by thin lines and the border of optimal colors by thick lines, respectively. The assumed light source is D65.

Quantization of the color gamut of the printers requires slightly less effort than quantization of the RGB space. The digitization for the two proofing processes sums up to the same order as that derived for the thermal dye sublimation printer (see Section 6.3.1), that is, 7-bit for the lightness and 8-bit for the a^* and b^* signals.

SUMMARY AND DISCUSSION

The CIELAB color space within the limit of optimal colors has been discussed and presented in graphical form by plotting planes of constant lightness L^* with a net of lines parallel to the a^* and b^* axes. These planes and the net of $a^* - b^*$ lines has afterwards been transformed into the CIE XYZ, into a standardized tristimulus RGB, a predistorted R′G′B′ space, and the YCC color space of the Photo CD. The planes of constant lightness with the net of $a^* - b^*$ lines uniform in the CIELAB space appear distorted after transformation into the various other color spaces. The distortion and compression of $L^*a^*b^*$ cells points to the areas of low or high sensitivity with respect to the color difference perception given in ΔE_{ab} units. In general, the most sensitive areas are found at the border of optimal colors in the green to yellow range depending on their lightness. In the CIE XYZ space, the most sensitive areas are located at low lightness, which follows directly from the definition of the CIELAB formula. In the tristimulus and distorted RGB spaces, the dependence on lightness is not that simple and sensitive areas with respect to color difference perception are found at low and medium lightness. The planes of constant lightness in predistorted color spaces are bowed.

To gain more insight into the valuation of color differences with the CIELAB formula, the color spaces considered have been quantized into a uniform grid of points and the grid has then been transformed into the CIELAB space, where it has become distorted. Maximum color differences between adjacent points of the grid in CIELAB coordinates have been calculated as a function of hue angle, lightness, and relative chroma to get a feeling for the distribution and variations of color differences and maximum values when switching color in digital steps. Around each test point considered in a quantized color space, the color differences to neighboring quantized points depend on the direction in the color space and a maximum color difference (worst color quantization step) is always found for one of the directions of digital steps. If the worst quantization steps along lines of test points at constant lightness are plotted for the chroma values of optimal colors or along chroma values defined by the RGB components of a positive RGB cube, variations of 1:3 to 1:6 are found in all the color spaces considered if the CIE 1976 formula ΔE_{ab} is used for the valuation of color differences. Still higher variations up to 1:25 are observed for the maximum quantization step within each plane of constant lightness versus lightness L^*. The largest color quantization steps are always found at the border of the color spaces. Much smaller variations appear if the new color difference formula CIE 1994, ΔE^*_{94} is used. In this formula, quantization steps of chroma are valued much less if chroma values are high.

Predistortion of color spaces based on RGB components reduces the color quantization steps preferably on the range of low lightness. Peak color quantization steps in the range of medium lightness are, however, not sufficiently affected by predistortion for the case of the optimal color space if the CIE 1976 formula ΔE_{ab} is used. Only for the smaller color spaces on

the basis of RGB components within a positive cube, predistortion results in essential advantages. This is demonstrated for the case of the YCC color space, where maximum color quantization steps of 16.5 are found for the standard 8 + 8 + 8 bit quantization concept if colors within a gamut of optimal colors or close to an optimal color boundary are considered. For colors limited to the positive RGB cube, the maximum quantization steps in the YCC color space are reduced to the order of 2 to 5. If the CIE 1994 formula is used as a basis for color difference calculation, the predistortion results in essential advantages compared to a linear RGB space.

Suitable quantization concepts for color spaces have been derived in this article from the maximum color quantization step found in each color space. The number of required bits per component has been derived on the condition of keeping the maximum color quantization step just equal to or below a value of 1. For the quantization of the CIELAB space itself, the $L^*a^*b^*$ axes have to be digitized into 8 + 9 + 9 bits = 26 bits. Many more bits are required for the CIE XYZ optimal color space (13 + 13 + 12 bits = 38 bits) on the basis of the CIE 1976 color difference formula, the tristimulus RGB optimal color space (13 + 12 + 12 bits = 37 bits), and the predistorted R′G′B′ optimal color space (12 + 12 + 12 bits = 36 bits). For the limitation of RGB components to the positive cube, 11 + 12 + 12 bits = 35 bits are required in tristimulus RGB components and 9 + 9 + 10 bits = 28 bits for the predistorted R′G′B′ space. If the positive RGB cube is transformed and quantized in CIELAB coordinates, only 8 + 8 + 8 bits = 24 bits are sufficient. Calculation of quantization on the basis of the CIE 1994 formula results in less effort in most cases (12 + 12 + 11 bits for the tristimulus RGB optimal color space, 10 + 10 + 9 bits for the predistorted RGB optimal color space, 11 + 12 + 11 bits for the positive RGB cube, and 9 + 9 + 9 bits for the predistorted positive RGB cube).

The quantization concepts as derived in this article lead to more conservative results than those published in previous work. In Kasson and Plouffe [1992], the quantization error defined as the average statistical quantization error and the three-sigma error has been calculated for a number of color spaces assuming quantization into 8 bits per component. For quantization of the CIE XYZ space, the average three-sigma error results in 4, for the CIELAB space 0.5 is given, and for the SMPTE-C/2.2 color space (predistorted R′G′B′ space with gamma = 2.2) a value of 2 results. Approximately, the reduction of the average error by the factor of 2 requires 1 bit more per component. On the basis of this relation, the CIE XYZ space would require 30 bits, the CIELAB space 21 bits, and the SMPTE space 27 bits. For further comparison with the results in this paper, it has to be considered that a mixture of valuation by the CIELAB and CIELUV color difference formula has been used in Kasson and Plouffe [1992] and the gamut of surface colors is a bit smaller than that of optimal colors. The latter might be the reason for less effort in the quantization of the CIELAB space derived in Kasson and Plouffe [1992] (7-bit difference).

The main difference of the results comes from the use of statistically averaged values compared to the use of peak values in this article. As

shown here, peak values of color differences by quantization effects deviate strongly from average values and hence, even the use of a three-sigma error leads to smaller bit numbers. Only for the case of the predistorted R′G′B′ color space, do the results in this article come to the same order as those published in Kodak [1992] for the SMPTE space (1-bit difference). In Stokes et al. [1992a], the necessary quantization of a predistorted R′G′B′ space for the control of cathode ray tubes has been estimated by 7.4 bits per component or 22 bits in total, also assuming a threshold limit of the order of 1. This comes close to the results of 23 bits derived in this article. Again, the published result is based on the statistical averaging of quantization effects, but the variation of color quantization steps for the positive R′G′B′ space (see Figure 25) has been found to be comparatively small.

The question of whether a quantization concept should be based on averaged values or peak values cannot be answered generally. It would help to investigate experimental data on the perceptible thresholds of the specific colors in the sensitive areas of a color space, where peak color quantization steps appear.

The studies on quantization effects have also been applied to a number of print processes (thermal dye sublimation, Chromalin, and Match Print). The device-dependent color spaces of these processes have been developed from measured data and plotted in $L^*a^*b^*$ coordinates. Due to their small color gamut, the quantization into 7 + 8 + 8 bits is sufficient to keep the maximum color quantization steps below 1. If the same gamut of colors is represented in tristimulus RGB components, 31 bits are required for the same precision, if ΔE_{ab} is considered.

With the assumption of a just-noticeable threshold of color perception of $\Delta E_{ab} = 1$, a rough estimation of the number of distinguishable colors included in the optimal color space results in $3.2 \cdot 10^6$. The same kind of estimation results in $1.1 \cdot 10^6$ just-noticeable colors included in a positive RGB cube, and the order of 0.45 to $0.48 \cdot 10^6$ is found for the color spaces of technical print processes, respectively. Hence, practical prints resolve only about 1/7 of the whole number of surface colors.

The comparison between the CIELUV and the CIELAB space by valuating the color differences in the CIELUV space by the CIELAB color difference demonstrates a strong inconsistency between both color difference definitions, particularly in the range of blue and green colors. If color differences are calculated with the CIE 1994 formula, a good match to the worst case color differences of the CIELUV space is found for all colors of high lightness. Only in the range of low lightness, strong differences still appear. The new color difference formula CIE 1994 is considered to describe color difference perception more consistent with experimental results. All the curves describing the distribution of color difference steps outlined in this article appear more uniform on the basis of this formula and result in lower numerical values in most cases. This is certainly an advantage for practical applications, even if the difficulty now is that the representation of colors in the established CIELAB space is not more consistent with uniform color difference valuation.

REFERENCES

ALMAN, D. H. 1993. CIE Technical Committee 1-29. Industrial color difference evaluation. Progress report. *Color Res. Appl. 18*, 137–139.

CCIR. 1982. CCIR Recommendation 601-1. Encoding parameters of digital television for studios. Geneva 1982–1986.

CCIR. 1990. CCIR Recommendation 709 (1990). Basic parameter values for the HDTV standard for studio and for international programme exchange. Geneva.

CIE. 1986a. Colorimetry. CIE Pub. 15.2, 2nd ed., Commission International de L'Eclairage, Vienna, 29–30.

CIE. 1986b. Colorimetry. CIE Pub. 15.2, 2nd ed., Commission International de L'Eclairage, Vienna, 30–31.

CIE. 1986c. Colorimetry. CIE Pub. 15.2, 2nd ed., Commission International de L'Eclairage, Vienna, 56–58.

CIE. 1993. Parametric effects in color-difference evaluation. CIE Pub. 101, Commission International de L'Eclairage, Vienna.

CIE. 1995. Industrial color-difference evaluation. CIE Pub. 116, Commission International de L'Eclairage, Vienna.

KASSON, M. J. AND PLOUFFE, W. 1992. An Analysis of Selected Computer Interchange Color Spaces. *ACM Trans. Graph. 11*, 4 (Oct.), 373–405.

KODAK. 1992. Photo CD products 1992. A planning guide for developers. Kodak Part Number DCI-200RJ Rochester, NY.

LANG, H. 1978. *Farbmetrik und Farbfernsehen*. Oldenbourg, Munich.

LANG, H. 1995. *Farbwiedergabe in den Medien, Fernsehen, Film, Druck*. Muster-Schmidt Verlag, Göttingen, Zürich.

LOO, M. R. AND RIGG, B. 1987. BFD (l:c) colour-difference formula. Part 1: Development of the formula. *JSDC 103* (Feb.), 126–132. Part 2: Performance of the formula. *JSDC 103* (March), 86–94.

MACADAM, D. L. 1935a. The theory of the maximum visual efficiency of color materials. *J. Opt. Soc. Am. 25*, 249.

MACADAM, D. L. 1935b. Maximum visual efficiency of color materials, *J. Opt. Soc. Am. 25*, 361.

MAHY, M., MELLAERT, B. V., AND VAN EYCKEN, O. A. 1991. The influence of uniform color spaces on color image processing: A comparative study of CIELAB, CIELUV, and ATD. *J. Imag. Technol. 17*, 5 (Oct.), 232–243.

POINTER, M. R. 1980. The gamut of real surface colours. *Color Res. Appl. 5*, No. 3, 145–155.

RICHTER, M. 1979. *Einführung in die Farbmetrik. 2. Auflage 1981*, de Gruyter, New York.

RÖSCH, S. 1929. Darstellung der Farbenlehre für die Zwecke der Mineralogie, *Fortschr. Mineral. Krist. Petrogr. 13*, 143.

SAE. 1985. SAE J 1545 1985. Recommended practice, instrumental color difference measurement for exterior finishes, textiles, and colored trim. SAE.

SCHRÖDINGER, E. 1920. Theorie der Pigmente von größter Leuchtkraft, *Ann. Physik (IV) 62*, 603.

SCHWARZ, M. W., COWAN, W. B., AND BEATTY, J. C. 1987. An experimental comparison of RGB, YIQ, LAB, HSV, and opponent color models. *ACM Trans. Graph. 6*, 2 (April), 123–158.

STOKES, M., FAIRCHILD, M. D., AND BERNS, R. S. 1992a. Precision requirements for digital color reproduction. *ACM Trans. Graph. 11*, 4 (Oct.), 406–422.

STOKES, M., FAIRCHILD, M. D., AND BERNS, R. S. 1992b. Colorimetrical quantified visual tolerances for pictorial images. In Techn. Association of the Graphic Arts, TAGA Proceedings, vol. 2, M. Pearson Ed., 357–777.

Received June 1994; revised November 1996; accepted January 1997